Disruption of Tomato TGS Machinery by ToLCNDV Causes Reprogramming of Vascular Tissue Specific TORNADO1 Gene Expression

Shreya Chowdhury
Bose Institute Division of Plant Biology
Shrabani Basak
Bose Institute Division of Plant Biology
Rohit Das
Bose Institute Division of Plant Biology
Arunava Mandal
Bose Institute Division of Plant Biology
Pallob Kundu (pkundu@jcbose.ac.in)
Bose Institute https://orcid.org/0000-0003-4272-945X

Research Article

Keywords: Tomato, Leaf vein, ToLCNDV, Leaf Curl, DNA methylation, Gene silencing, Disease symptom, Transgenic, Transcription, Reporter assay

Posted Date: August 30th, 2021

DOI: https://doi.org/10.21203/rs.3.rs-660321/v1

Title: Disruption of tomato TGS machinery by ToLCNDV causes reprogramming of vascular tissue specific *TORNADO1* gene expression

Authors and Affiliation:

Shreya Chowdhury, Division of Plant Biology, Bose Institute, P1/12 CIT Scheme VIIM, Kolkata,700054, West Bengal, India. shreyachowdhury13@gmail.com

Shrabani Basak, Division of Plant Biology, Bose Institute, P1/12 CIT Scheme VIIM, Kolkata, 700054, West Bengal, India. shrabani187@gmail.com

Rohit Das, Division of Plant Biology, Bose Institute, P1/12 CIT Scheme VIIM, Kolkata, 700054, West Bengal, India. rohitdas@jcbose.ac.in

Arunava Mandal, Department of Genetics, University of Calcutta, 35 Ballygunge Circular Road, Kolkata, 700019, West Bengal, India. amgntcs@caluniv.ac.in

Pallob Kundu, Division of Plant Biology, Bose Institute, P1/12 CIT Scheme VIIM, Kolkata, 700054, West Bengal, India. pkundu@jcbose.ac.in

Disruption of tomato TGS machinery by ToLCNDV causes reprogramming of vascular tissue specific *TORNADO1* gene expression

Shreya Chowdhury[1], Shrabani Basak[1], Rohit Das[1], Arunava Mandal[2] and Pallob Kundu[1],*

[1]Division of Plant Biology, Bose Institute, P1/12 CIT Scheme VIIM, Kolkata, 700054, pkundu@jcbose.ac.in

[2]Current address, Department of Genetics, University of Calcutta, 35 Ballygunge Circular Road, Kolkata, 700019

*, author for correspondence

Key message: Vascular development-related *TRN1* transcription is suppressed by cytosine methylation in growing leaves of tomato. ToLCNDV infection disrupts methylation machinery and reactivates *TRN1* expression - likely leading to symptom manifestation.

Key words: Tomato; Leaf vein; ToLCNDV; Leaf Curl; DNA methylation; Gene silencing; Disease symptom; Transgenic; Transcription; Reporter assay

Declaration:

Funding: Supproted by INSPIRE Fellowship from DST to Shreya Chowdhury and Bose Institute Intramural fund to Pallob Kundu

Conflict of interest: Nothing to declare

Availability of data and material: All data are included in the manuscript and supplementary materials. Other materials will be made available on request.

Code availability: Not applicable

Authors contribution: SC and PK designed all experiments. SC performed all experiments. SB, RD and AM provided some reagents and assisted in conducting the experiments. SC and PK wrote the paper. All authors have seen the manuscript, provided input and confirmed submission.

Ethics approval: Not applicable.

Consent to participate: Not applicable

Consent for publication: Obtained from all authors.

Abstract:

Leaf curl disease of tomato caused by Tomato Leaf Curl New Delhi Virus (ToLCNDV) inflicts huge economical loss. Disease symptoms resemble leaf developmental defects including abnormal vein architecture. Leaf vein patterning related *TORNADO1* gene's (*SlTRN1*) transcript level is augmented in virus-infected leaves. To elucidate the molecular mechanism of the upregulation of *SlTRN1* in vivo we have deployed *SlTRN1* promoter-reporter transgenic tomato plants and investigated the gene's dynamic expression pattern in leaf growth stages and infection. Expression of the gene was delimited in the vascular tissues and oppressed in growing leaves. Methylation-sensitive PCR analyses confirmed the accumulation of CHH methylation at multiple locations in the *SlTRN1* promoter in older leaves. However, ToLCNDV infection reverses the methylation status and restores expression level in the leaf vascular bundle. The virus dampens the level of key maintenance and *de novo* DNA methyltransferases *SlDRM5*, *SlMET1*, *SlCMT2* with concomitant augmentation of two DNA demethylases, *SlDML1* and *SlDML2* levels in *SlTRN1* promoter-reporter transgenics. Transient overexpression of *SlDML2* mimics the virus-induced hypomethylation state of the *SlTRN1* promoter in mature leaves. Further, in line with the previous studies, we confirm the crucial role of viral suppressors of RNA silencing AC1 and AC4 proteins in promoting DNA demethylation and directing it to reinstate activated transcription of *SlTRN1* in silenced tissues for possible modification of leaf venation architecture, leaf curling and easy vector acquisition of viral particles.

Introduction:

Persistent multiplication of Tomato Leaf Curl New Delhi Virus (ToLCNDV), a whitefly transmitted *begomovirus,* in tomato causes one of the frugally important diseases known as leaf curl, resulting in constrained tomato production. The symptoms include upward or downward leaf curling, vein swelling, leaf wrinkling, and blistering with stunted and shortened internodes, somewhat mimicking leaf developmental defects. Reduced production and fruit rotting at later stages limit crop yield. ToLCNDV is a bipartite begomo virus with two similar-sized genomic components, DNA-A and DNA-B. The DNA-A component contains six open reading frames recognized as AC1, AC2, AC3, AC4, AV1, and AV2 (correspondingly C1, C2, C3, C4, V1 and V2 for monopartite begomovirus) encoding six proteins that help in virus replication, viral gene

transcription, pathogenesis, and encapsidation while the DNA-B has two ORFs (BC1 and BV1) required for virus movement and transmission. Genetic resistance in cultivated varieties is not common, thus, major virus management measures include whitefly control and avoidance of most susceptible cultivars. For better management, many studies are still required to understand the disease biology and causes of the typical symptom manifestation.

The development of symptoms in a host plant by a geminivirus depends on the plant type infected. Scientists have identified numerous host factors which play a pivotal role in shaping the degree of disease severity. To analyze the host response towards individual viral proteins, six open reading frames of Tomato leaf curl virus (TLCV) were transiently expressed in *Nicotiana* plants (Gorovits et al. 2017). In *N. benthamiana*, the C4 gene produced leaf curl symptoms in all plants infected while the products of V1 and C3 triggered stunting only. Many viral proteins interact with host factors. BC1 interacts with tomato AS1, a Myb transcription factor, altering leaf development encompassing lamina symmetry, venation patterning, and leaf dorsiventrality (Yang et al. 2008). In one such study, (Mandal et al. 2015) from this laboratory, of a gene being regulated in infection the *TORNADO1* (*TRN1*) encoding a conserved plant-specific signaling protein having a role in leaf vein patterning processes, was shown to be upregulated. These studies suggest multifaceted interactions between viral genes and host factors modulate symptom development in plants.

SlTRN1 or *Solanum lycopersicum TORNADO1* is a plant-specific protein of 1456 amino acids with a high analogy to NOD-LRR proteins and cytoplasmic locations. It resembles 'R' genes in plant pathogen resistance with the presence of both NBS and LRR domains, suggesting a role of TRN1 in signalling. TRN1 together with the AS1 (Asymmetric leaves1) play role in leaf venation patterning and lateral symmetry formation. TRN1 facilitates auxin channelization for procambium cell formation leading to the differentiation of xylem and phloem cells. *trn1* mutants show altered vascular pattern formation and root development suggesting its role only in early leaf and root development (Cnops et al. 2006). Here we report that *TRN1* expression level is negatively correlated to leaf maturity, and the gene's expression is suppressed by the epigenetic mechanism in a fully grown leaf. Since the overall expression level of *SlTRN1* is increased during infection, we have questioned whether viral proteins or replication could reverse methylation-mediated gene silencing in infected plants.

Epigenetic regulation of gene expression via DNA methylation plays a significant role in the silencing of genes whose function is not required at a specific stage of tissue development. DNA methylation signifies the addition of a methyl group in the C5 position of cytosine, forming 5-methylcytosine (5-mC), is an important epigenetic mechanism triggering gene silencing, transposable element silencing, X-chromosome inactivation, genome stability, and genomic imprinting. DNA methylation in plant promoters leads to the negative regulation of various genes' expression crucial in plant growth and development (Bartels et al. 2018). In plants, mammals, and some fungi DNA methylation occurs in the CG region which is an evolutionarily conserved phenomenon. In higher plants, in addition to CG methylations, DNA methylation also occurs in CHG (symmetric) and CHH (asymmetric) contexts (H=A, C, or T). In Arabidopsis, DNA methyltransferase1 (MET1), an ortholog of Dnmt1 in mammals, maintains CG methylations. Chromomethylase 2 and 3 (CMT2 and CMT3) and the de novo DNA methyltransferases Domains rearranged methyltransferase 1 and 2 (DRM1 and DRM2) are mainly responsible for DNA methylations at CHG and CHH contexts. A classical example of methylation-mediated inhibition of gene expression is repression of WUSCHEL (Li et al. 2011). DNA methyltransferases CHROMOMETHYLASE 3 (CMT3) or METHYLTRANSFERASE 1 (MET1) hypermethylated WUSCHEL and inhibited its expression. Cytokinin-induced demethylation restores the gene's expression and shoots initiation (Liu et al. 2018). Another example, DNA hypermethylation of the ERECTA family genes leads to defects in stomatal development (Wang et al. 2016).

DNA methylation acts as a steady genetic mark, i.e. once the methyltransferase adds the methylation on DNA, it remains there. However, CHH methylation is termed 'non-symmetrical' as during DNA replication the opposite strand lacks a methylated cytosine and *de novo* methylation needs to be established after each replication cycle (Moglia et al. 2019). DNA demethylation can act both actively by removing 5-methyl cytosines by the base excision repair pathway (BER) or passively during DNA replication when a newly synthesized strand remains unmethylated or is not methylated by DNA methyltransferases. The two DNA demethylases DEMETER (DME) and REPRESSOR OF SILENCING 1 (ROS1) encodes a DNA glycosylase and can dynamically eliminate the methylations through the BER pathway. Mutations in them can cause enhanced DNA methylations in all genomic contexts. Cytosine methyltransferases

mutants of *Arabidopsis* show hypersusceptibility to geminivirus infections because of the inability to methylate viral DNA (Raja et al. 2008).

RNA silencing is the major antiviral mechanism found in all higher plants (Ruiz-Ferrer and Voinnet 2009; Ding 2010; Llave 2010). Several studies suggest post-transcriptional gene silencing (PTGS) is activated against RNA viruses and transcripts produced by DNA viruses such as geminiviruses (Rodríguez-Negrete et al. 2013). Upon virus infections, double-stranded RNA molecules of viral origin are processed into small interfering RNAs (siRNAs) by the action of dicer-like proteins (DCL2, DCL4) (Elbashir et al. 2001) which mediate PTGS. Some other 24 nucleotide siRNAs, processed by DCL3, cause transcriptional gene silencing (TGS) or RNA-induced transcriptional silencing (RITS) by methylating viral DNA thus hindering its replication. To counter the plant defense mechanism viral proteins are evolved to interfere with the plant methylation machinery (Díaz-Pendón and Ding 2008; Raja et al. 2008). Some of the viral suppressors of RNA silencing (VSR) include viral AC2 determined TrAP (Wang et al. 2003), AC4 protein (Vanitharani et al. 2004), and V2 protein (Luna et al. 2017). The VSRs act at numerous steps of the RNA silencing pathway thereby distressing the host defense mechanism. AC2 acts as a TGS suppressor by two mechanisms which include, (i) adenosine kinase inhibition (Wang et al. 2003); and (ii) reduction of proteasome-mediated degradation of S-adenosyl methionine decarboxylase1 (Zhang et al. 2011). Some of the targets of VSRs such as AGO4 and methyltransferases like MET1, CMT3, DRM1, and DRM2 are required for methylating viral DNA. AC4 protein interacts with AGO4 and influences cytosine methylation of the viral genome (Vinutha et al. 2018). Reports suggest AC2 protein hinders the production of S-adenosyl methionine which is a methyltransferase cofactor (Buchmann et al. 2009). Replication-associated protein (Rep) deters the expression of two key methyltransferases MET1 and CMT3 (Rodríguez-Negrete et al. 2013). Lessening of activities of methyltransferases may lead to fall of global methylation in the genome including promoters, thus, misregulation of multiple genes.

This study delved into the molecular mechanism of reversible DNA methylation on *SlTRN1* promoter during ToLCNDV infection. We show that AC1 and AC4 play a vital role in the suppression of the levels of maintenance and *de novo* DNA methyltransferases leading to transcriptional gene silencing reversal and re-activation of naturally silenced *SlTRN1* in mature leaves of tomato. VSRs-mediated misregulation of this crucial developmental gene could cause some of the typical symptoms of the disease.

Materials and methods:

2.1 Plant Material:

Throughout the study we have used tomato (*S. lycopersicum* L.) cultivar Pusa Ruby, originally released by IARI, New Delhi. Seeds were regularly procured from Sutton Seeds, India and also propagated in in-house facility. Experimental plants were grown in glass houses at 25^{o}C ± 2 with natural light and humidity in plastic pots containing Soilrite (Keltech Energies Ltd, India) supplemented with Suphala fertilizer (N, P and K each at 15% by weight). For specific experiments leaves were categorized based on their length as small (0.2-1.0 cm, upto 10 days), medium (1.1 cm-2.5cm, 10-20 days) and large (2.6-4.5cm, 20-30 days).

2.2 Agrobacterium-mediated plant transformation:

Agrobacterium-mediated transformation of tomato cotyledonary leaf explants were carried out using standard methodology. In brief, explants were collected from 7 days old healthy seedlings grown in solid MS medium (MS salts and 3% sucrose) under aseptic condition. *Agrobacterium tumefaciens* LBA4404 strain harbouring *SlTRN1* (Solyc03g112750.2) promoter fragment GUS gene fusion in pCAMBIA1304 binary vector (Supplementary Fig. 1A,-344/+UTR, (Mandal et al. 2015) was used to transform tomato explants. Agrobacterium culture was grown in LB media supplemented with 50mg/l Kanamycin and 50 mg/l Rifampicin at 28^{o}C by continuous shaking for 48 h. Cells were harvested by centrifugation at 4^{o}C, re-suspended in MS medium supplemented with 100µM acetosyringone and adjusted to a final OD_{600} of 0.8. Cotyledonary leaves were excised of tip and petiole, and pre-incubated in MS medium supplemented with 0.1 mg/l NAA and 1 mg/l Zeatin for 2 days at 25^{o}C under 16/8 h light–dark cycles. Explants were immersed in Agrobacteria suspension for 30 min with occasional shaking and returned to the same preincubation media after removal of excess liquid. Following two days of co-culture at 25^{o}C under 16/8 h light–dark cycles the explants were transferred to regeneration media (MS medium, 0.1 mg/l NAA, 1 mg/l Zeatin, 250 mg/l cefotaxime and 10 mg/l hygromycin) and incubation was carried out till callus induction. Calli were maintained on 25 mg/l hygromycin containing media until shoot development was observed. Emerged shoots were detached from the callus and transferred to rooting media (MS medium, 250 mg/l cefotaxime and 10 mg/l

hygromycin) in jam bottles. Plantlets with profused roots were selected. Finally, the plants were transferred to soilrite and kept under moist condition in culture room for hardening. Transgenic plants were planted in larger pots and maintained in glass houses for seed production.

2.3 Selection of T_1 generation seeds:

Seeds obtained from transgenic T_0 plants were surface sterilized with 30% commercial bleach and 0.05% Triton X 100 solution, followed by repeated washing in autoclaved water till the smell of bleach disappeared. Then the seeds were germinated on MS media supplemented with 25 mg/l Hygromycin. The germination rate of 90-95 % was routinely obtained; however, selection rate differed in different lines.

2.4 Transient Agroinfiltration of tomato leaves:

Agroinfiltration technique was used to infect tomato plants with ToLCNDV and also for transient gene expression assays. *A. tumefaciens* LBA4404 strain harboring clones of ToLCNDV-A (GenBank: DQ629101.1) and ToLCNDV-B (GenBank: DQ169057) genomes (LBA4404:ToLCNDV) were used for infection. Actively growing bacteria were harvested by centrifugation at 4000Xg at 4^{o}C, following which pellet was resuspended in MES buffer (10 mM MES and 10 mM MgCl2, pH 5.6) supplemented with 100µM acetosyringone and adjusted to a final OD_{600} of 0.8. Abaxial surfaces of 3 to 4 fully expanded leaves from about 20 days old plants were infiltrated at multiple spots with approximately 100µl of bacterial suspension in each spot, using 1 ml plastic syringe. Inoculated plants were maintained in glass house until symptoms appeared (~30 days). Similar protocol was employed to perform promoter activity assays with different constructs cloned in binary vectors pCAMBIA1304 or pPZPY112. About 40 days old plants were used for promoter activity assays. Plants agroinfiltrated with the empty vector were used as control in all experiments.

2.5 Histochemical GUS staining:

The β-glucuronidase (GUS) reporter gene activity in tissues was detected by GUS staining assays. Standard assays were performed with 5-bromo-4-chloro-3-indolyl β-D-glucoronide (X-gluc) as the substrate. The reaction buffer consisted of 50mM sodium phosphate buffer (pH 7),

1mM EDTA and 0.1% Triton-X100.Tissues were immersed in the buffer and incubated at 37^{o}C in dark for 6-10 hours with intermittent shaking and monitoring.The samples were then fixed in a fixative solution consisting of 70% ethanol, 5% acetic acid, 5% formaldehyde and 20% water for 30 minutes in room temperature. Subsequently, chlorophyll was removed by repeated washing with a solution consisting of glacial acetic acid, ethanol and glycerol in 3:1:1 ratio and photographed using a camera (Cannon) on a compound microscope (Leica).

2.6 Measuring physiological parameters of the plant:

A number of physiological parameters such as leaf stomatal conductance, atmospheric pressure, net photosynthetic rate, internal CO_2, transpiration rate, vapor pressure deficit etc. were measured using a Cl-340 Handheld Photosynthesis Analyzer (CID Bio-Science). Data was collected from multiple samples, average values were compared.

2.7 Total DNA Isolation and PCR analysis:

Total DNA was isolated from leaves using Plant DNAzol reagent (Invitrogen) following manufacturer's protocol. In brief, leaf tissues were pulverized in liquid nitrogen, and the powdered tissues were suspended in Plant DNAzol reagent (0.3 ml for 0.1g plant tissue) supplemented with RNAse A (100µg RNAseA/ml Plant DNAzol), mixed by gentle inversion and incubated at 25^{o}C with shaking for 5 min. To the mixture 0.3ml chloroform was added, mixed well and centrifuged at 12,000g for 10min. DNA was precipitated with 100% cold ethanol from the aqueous phase and finally resuspended in TE buffer (10 mMTris-HCl pH 8.0 and 1 mM EDTA).Viral coat protein and movement protein specific PCRs with ND-F/ND-R and BC-F/BC-R primer sets (Supplementary Table 3), respectively, and using total DNA isolated from newly emerged leaves were carried out to screen infected plants.

2.8 Total RNA Isolation and RT-PCR analysis:

Total RNA was prepared from ~500 mg tissue of mock-infected (control) plants and systemic ToLCNDV infected leaves by TRIzol reagent (Invitrogen) following manufacturer's protocol. To eliminate contaminating DNA the RNA samples were treated with RNase-free DNaseI (20 U/µg of DNA, Fermentas, USA) for 1 h at 37^{o}C and RNA was further purified by phenol–chloroform extraction followed by ethanol precipitation using standard protocol. RNA integrity

was checked by resolving the isolated RNA in a 1.5 % Agarose-TAE gel. Complementary DNA was prepared from RNA samples that had distinct 28S and 18S bands showing approximately 2:1 intensity ratio. Five microgram total RNA was reverse-transcribed to make cDNA using 200 U RevertAid reverse transcriptase (Thermo scientific) with random hexamer (5 µM) primers in a total reaction volume of 20 µl, following manufacturer's protocol.

cDNAs were two-fold diluted with sterile water and 1µl was used as template in each 20µl reaction of SYBR green based real time PCR using Applied Biosystems 7500 FAST machine. Three technical replicates were analyzed for each sample of cDNA. Mock infiltrated plants' cDNA served as control. Amplification of specific products was confirmed by obtaining a single peak in melt curve analysis, first derivative of fluorescence (dF/dT) versus temperature plot. The expression level of the gene of interest, normalized to the level of EF1α and relative to the expression at control (described in individual experiment), was calculated for each sample using the $2^{-\Delta\Delta cT}$ method.

2.9 GUS Activity assay:

Leaf tissues (~3 sq cm) from Agroinfiltrated zones or transgenic plants were collected in a 1.5ml centrifuge tube and grinded with liquid nitrogen. Powdered tissues were suspended in 500 µl of GUS extraction buffer (50 mM NaHPO4, pH 7; 10 mM 2-mercaptoethanol; 10 mM Na_2EDTA; 0.1% SDS; 0.1% triton X-100) and incubated on ice for 10 min. The mixture was centrifuged at 15,000 g for 10 min at 4^{o}C and clarifiedsupernatantwas collected for leaf protein extracts. 50µl of protein extract was mixed with 250µl of GUS assay solution (2 mM 4-methyl umbelliferyl-d-glucuronide in extraction buffer),incubated at 37^{o}C for 60 min and proceeded to fluorescence measurement (excitation at 365 nm and emission at 455 nm, readings were taken for 5 sec) using Varioskan flash multimode plate reader (Thermo scientific, Finland). An aliquot of the same protein extract was diluted 50 times and concentration was determined using Bradford reagent (Himedia, India). Data was normalized based on the protein concentration of each sample.

2.10 Full length cloning of CDS of DNA-demethylase gene:

Full length DNA demethylase (Solyc10g083630.1.1) coding sequence was amplified from tomato cDNA pool using gene specific primers (Supplementary table 3) and a high fidelity Polymerase (KOD FX Neo, Toyobo). The 5.5 kb amplified product was gel-purified and cloned

in pCAMBIA1304 binary vector utilizing the *Nco*I and *Bst*EII sites downstream of the CaMV35S promoter. Positive clones were mobilized into *A. tumefaciens* LBA4404 for expression studies in plant.

2.11 Methylation sensitive PCR analysis:

Total genomic DNA was isolated from transgenic infected and uninfected tomato plants using DNAzol reagent (Thermo Fisher Scientific). Purified 200ng DNA was digested using 10U of *Nla*III restriction enzyme (New England Biolabs), that cleaves only unmethylated sites, at 37^{o}C for 1h and enzyme inactivation at 65^{o}C for 1h was followed (Dasgupta and Chaudhuri 2019). PCR primers were designed on either side of four *Nla*III sites present in the promoter region of *SlTRN1* gene. The digested DNA used as template to perform 30cycles of 3 steps PCR (95^{o}C 30 sec, 58^{o}C 30 sec and 72^{o}C 30 sec) using Dream Taq DNA polymerase (NEB). Control reactions were performed with (i) undigested DNA of the same sample (no enzyme control) and (ii) amplification from a region devoid of *Nla*III site (no cut site control) using both undigested and digested DNA as templates. PCR products were resolved in 2.5% Agarose-TAE gel containing 1 µg/ml ethidium bromide and photographed.

2.12 Treatment of transgenic plants with a methylation blocker:

5-azacytidine was solubilized in 40% ethanol and 10 µM solution was freshly prepared prior to each application. One month old transgenic plant leaves were treated with 5-azacytidine for 20 days on both dorsal and ventral surfaces by topical application using a small cotton swab once a day. Control plants received only 40% ethanol solution. Multiple leaves of at least three biological replicates were treated for each experiment. DNA isolation and PCR reactions were carried out as mentioned above.

2.13 Software:

Primers were designed manually and OligoAnalyzer3.1 software from Integrated DNA Technologies (https://www.idtdna.com/pages/tools/oligoanalyzer) was used to analyze a new design. Quantity One Basic software from Bio Rad (www.bio-rad.com/en-uk/product/quantity-one-1-d-analysis-software) was used to quantify the intensity of PCR band products. Upstream sequences of *SlTRN1* gene was downloaded from SOL Genomics Network

(http://solgenomics.net/). These sequences were analyzed in MatInspector (Genomatix) to find putative cis-elements for transcription factor binding. NCBI BLAST was used for homology search and alignments.

2.14 Statistics:

We took three different plants of same age group in all experiments. Real time PCR analyses were performed with RNA preparations from three different plants and reactions were also done in triplicates. Results are expressed as means± standard deviation (SD). Two-tail Student's t-test was employed, if needed, and $p \leq 0.05$ considered as significant. We have also performed two-way ANOVA test when essential and $p \leq 0.05$ considered as significant.

Results:

3.1 *SlTRN1* expression is restricted to all vascular tissues of tomato:

TRN1 is linked to vein development in Arabidopsis (Cnops et al. 2006) and we have previously confirmed *SlTRN1* expression in growing leaves of tomato (Mandal et al. 2015). Therefore, we asked whether tomato TRN1 is also vascular tissue specific. For precise monitoring of the in vivo expression pattern we have developed *TRN1* promoter-reporter transgenic lines (TRN1-GUS) using -344/+UTR-GUS which is one of the best studied promoter construct (Mandal et al. 2015) (Supplementary Fig. 1A). Five transgenic lines derived from separate callus were selected for subsequent experiments (Supplementary Fig. 1B). Amplification of a distinct band in *hptII* gene-specific PCR performed with genomic DNA isolated from leaf of these lines confirmed transgene integration (Supplementary Fig. 1C). Absence of significant amplified products in control PCRs performed with vector backbone specific primers and from wild type plants, nullified the possibility of amplification from contaminating Agrobacterium. These plants were also expressing GUS transcripts in comparable level (Supplementary Fig. 1D). Seeds of transgenic plants were germinated on 25mg/l Hygromycin containing media prior to transfer to soil for propagation. Germination frequency of 90-95% of T_0 plants was obtained, hinting insertion of multiple T-DNAs. Further experiments were performed with mostly T_2-generation plants. Plants of all lines were phenotypically indistinguishable from glasshouse grown wild type controls (Fig. 1A). Physiological parameters of transgenics were found to be equivalent to wild type controls (Supplementary Table 1).

Histochemical staining revealed the GUS gene expression pattern, resulting from *TRN1* promoter activity, in different vegetative parts (Fig. 1B, C). Stem, leaf and root showed expression level of GUS gene in descending order (Fig. 1D). To obtain a better idea about *TRN1* promoter activity in tissues transverse sections of stem and leaf were GUS-stained. As expected, GUS activity was restricted to the vascular tissues, including vascular interfascicular and intrafascicular cambium (Fig. 1E and F) and pericycle. Staining of longitudinal section of stem confirmed heightened GUS expression within vessels (Fig. 1G). Reproductive tissues also showed high GUS expression (Fig. 2), especially in veins. Hence, *TRN1* promoter is active in vascular tissues of vegetative as well as reproductive organs of tomato.

3.2 *TRN1* gene expression pattern changes with developmental stages of leaf and virus infection:

Vascular development and reticulation is correlated to leaf growth. We have previously reported that ToLCNDV infection causes increased TRN1 expression (Mandal et al. 2015).Thus, we intended to learn about *TRN1* expression pattern in leaf growth stages during infection. Transgenic plants were infected via agroinfiltration and incubated for one month for disease establishment (Fig. 3A). Infection resulted in stunted plant growth, curling of leaf and vein thickening with multiple open ends. Systemic infection was confirmed by virus coat protein (CP) and movement protein (MP) specific PCR analyses using total DNA isolated from leaves of uninfected and symptomatic plants (Fig. 3B). CP and MP genes were not detectable in control plants, indicating specificity of the reaction. Plants having significant infection, as indicated by prominent amplification of 750nt CP and 850nt MP amplicons, were selected for subsequent experiments. In line with our previous observation (Mandal et al. 2015) where we found augmentation of *SlTRN1* gene expression in ToLCNDV infection, GUS-activity was noticeably increased in leaves of all three lines tested (Fig. 3C) during the infection, with an average of 2.79±0.52 fold increase ($p \leq 0.05$) (Fig. 3C). Enhanced GUS-staining was also observed in infected roots (Fig 3D).

To scrutinize the variation of GUS activity in varied growth stages, we collected leaves of different sizes and for the simplicity of explanation grouped them into small, medium and large leaves. GUS expression pattern in uninfected and during infection was analyzed by both histochemical staining and fluorometric analyses. Interestingly, intensity of GUS-staining was

most in small leaves and gradual decrease in GUS activity was noticed with progression of leaf growth. The difference in average GUS activity between small and large leaf was almost 2.5±0.50 ($p \leq 0.05$) folds (Fig. 3E). Large leaves did not develop typical intense staining pattern, indicating suppression of *TRN1* gene expression occurs in a large leaf. However, ToLCNDV infection reinstated GUS-staining in large leaves, and slightly increased in growing leaves (Fig. 3E). The observation was corroborated by fluorometric assays performed with similar sets of leaves (Fig. 3F). GUS activity in small, medium and large leaves was increased in the order of 2.6±0.50 ($p \leq 0.05$), 3.06±0.29 ($p \leq 0.05$) and 3.49±0.45 ($p \leq 0.05$) fold, respectively during the infection. Tissue staining also indicated heightened GUS activity in vascular bundles of mature leaves, corroborating enhanced *TRN1* promoter activity during infection (Fig. 3G). These results hint that *SlTRN1* gene expression is tightly regulated during growth while virus disrupts the regulation pattern.

3.3 WRKY transcription factor mediates augmentation of transcription from *SlTRN1* promoter and GUS transgene expression

To investigate the mechanism of heightened GUS expression, we first analysed the GUS transcript level, which should provide information about the *TRN1* promoter activity. RT-dependent real-time PCR was carried out with GUS-specific primers. The analysis confirmed upregulation of GUS transcript level in all three lines tested (2 folds, $p \leq 0.05$, average of three lines) upon ToLCNDV infection (Fig. 4A). The promoter harbours two prominent W-boxes (Supplementary figure 1A) and we had previously shown that (Mandal et al. 2015) WRKY16 expression was increased during the infection and WRKY16 readily activated *SlTRN1* promoter. Here we show that Agroinfiltration of *WRKY16* into TRN1-GUS transgenic plants also activated the promoter, resulting 2.1± 1.1 folds ($p \leq 0.05$) upregulation of GUS transcript level (Fig. 4B), and 2.13± 0.45 folds ($p \leq 0.05$) and 2.29±0.16 folds ($p \leq 0.05$) increase in GUS activities in small and large leaves, respectively (Fig. 4C). Infiltration of a set of NAC transcription factors (Bhattacharjee et al., 2017) or treatment with abiotic stress had no effect (Supplementary Figure 2B). We have also checked the regulation of promoter under the influence of WRKY16 transcription factor during virus infection and found 1.55±0.09 folds ($p \leq 0.05$) upregulation of GUS activity in infection (Fig. 4E). Agroinfiltration of WRKY16 into infected leaves resulted in additional increment of GUS activity (from 1376.11 to 2144.09 pmole MU/µg protein/h; blue

bars, Fig. 4D), suggesting WRKY16-mediated transcriptional regulation can act synergistically to the infection, or an alternative mechanism of promoter regulation is activated during ToLCNDV replication.

3.4 Methylation pattern of *SlTRN1* promoter is regulated during growth and ToLCNDV infection

Differential DNA-methylation of the genome is an integral component of the regulation of gene expression in angiosperms. The exclusive expression pattern of *SlTRN1* gene in leaf developmental stages and also during ToLCNDV infection in transgenic plants prompted us to discern whether dynamics of promoter-methylation plays an important role in regulating the gene expression under different conditions. We opted for the methylation-sensitive PCR analysis to identify the cytosine methylation occurring in the promoter region of the *SlTRN1* gene. It harbours four CATG sequences, recognition site of *Nla*III restriction enzyme, within 500nt upstream to the translation start site (Fig. 5A, B). *Nla*III cleaves only unmethylated CATG sites (Guzmán-Benito et al. 2019). We have utilized this enzyme in methylation sensitive PCR analysis of genomic DNA isolated from different sizes of leaves of wild type plants, and uninfected as well as ToLCNDV-infected TRN1-GUS transgenic tomato plants. In wild type and uninfected samples, the band intensities of PCR products obtained from *Nla*III cut genomic DNA were varied in the order of large>medium>>small leaves (Supplementary Fig. 3A, Fig. 5C, left panel and Supplementary figure 4A). Hinting, methylations in all four sites were more common in larger leaves compared to the small and medium leaves. Intriguingly, meager amount of amplification was detected in *Nla*III digested infected samples (Fig. 5C, right panel), and greater inhibition of amplification was observed in samples collected from large leaves (Supplementary figure 4A). Thus, infection caused inhibition or removal of methylations in all four sites tested, in all sized leaves. Equivalent intensities of bands in no enzyme controls affirmed equal amount of DNA was used in each sample in this experiment. To confirm the integrity and quality of the DNA used in these experiments, we performed the no cut site control reactions with all enzyme-treated and no-enzyme-treated templates. The equal intensity of PCR products in each sample validates that high quality of the DNA was always used. Another control experiment was performed with a methylation specific enzyme, *Dpn*I, which lacks any restriction site in the promoter region. Observation of equal intensity bands in all enzyme-treated and no-enzyme-

treated templates confirmed specificity of methylation-sensitive PCR reactions (Supplementary Figure 3B). Collectively, these data show that *SlTRN1* promoter accumulates more methylation with aging of a leaf, while infection obliterates methylation marks at all tested sites, irrespective of the age of the leaf.

3.5 Treatment with a methylation blocker abolishes methylation marks at *Nla*III sites

To examine the effect of a methylation blocker on the promoter methylation we have treated plants with 5-azacytidine, which inhibits methyltransferase activity leading to hypomethylation of genomic DNA. Leaves of varied age were regularly smeared with either 5-azacytidine or the solvent only as placebo. *Nla*III digested and no enzyme control genomic DNA from placebo and treated plants were subjected to methylation-sensitive PCR analysis (Fig. 6A)(Böhmdorfer et al. 2014). In plants treated with methylation blocker, methylation marks were not detectable in any of the 4 *Nla*III sites, as observed by the absence of bands in treated and enzyme digested samples while in untreated samples the band intensity was increased from small to large leaves (Fig. 6A, right panel vs. left panel; Supplementary figure 4B). Control reactions were similar to that have been described in the previous section. Further, we investigated the effect of 5-azacytidine on promoter activation and performed histochemical GUS staining on placebo and treated leaves. Significant higher reporter activity in all categories of leaves was apparent (Fig. 6B), (2.87±0.13 ($p \leq 0.05$), 3.12±0.26 ($p \leq 0.05$) and 4.14±0.28 ($p \leq 0.05$) folds in small, medium and large leaves, respectively, while maximum activation occurred in larger leaves. Intense blue precipitation in 5-azacytidine treated large leaves compared to mock treated ones confirmed the recrudescence of promoter (Fig. 6C). These results further validating leaf maturity accelerates methylation at CATG sites in *SlTRN1* promoter leading to suppression of promoter activity and methylation blocker reverses the effect of such methylations.

3.6 Methyl transferase and demethylase expression pattern correlates with *SlTRN1* promoter methylation level in growing leaves and ToLCNDV infection

The differential level of methylations found in the promoter region of growing leaves as well as in virus infected plants hinted that altered regulation of DNA methyl transferases and/or DNA demethylase was responsible for such variation in methylation intensity. Hence, we set out to investigate the expression levels of some these genes during leaf growth. Interrogation of the

tomato genome yielded four DNA methlytransferases (*SlCMT4*, Solyc08g005400; *SlMET1*, Solyc11g030600; *SlCMT2*, Solyc12g100330 and *SlDRM5*, Solyc02g062740) which are homologous to Arabidopsis CHROMOMETHYLASE3 (CMT3), and DOMAINS REARRANGED METHYLTRANSFERASE 2 (DRM2). Three DNA demethylases (*SlDML3*, Solyc11g007580; *SlDML1*, Solyc09g009080 and *SlDML2*, Solyc10g083630) which are homologous to Arabidopsis DEMETER (DME) and REPRESSOR OF SILENCING1 (ROS1) were also identified (Supplementary table 2). RT-dependent quantitative PCR analysis was performed to detect the expression level of these genes in varied size of leaves of transgenic plants (Fig. 7A). Expression levels of 3 methyltransferases, *SlDRM5*, *SlMET1*, and *SlCMT2* were significantly more in large leaves, 4.20±0.56 ($p \leq 0.05$), 4.80±1.14 ($p \leq 0.05$) and 2.66±0.85 ($p \leq 0.05$) fold, respectively, compared to small leaves. Concomitant decrease in expression level of three Demethylases (*SlDML3*, *SlDML1*, and *SlDML2*), in the order of 5.32±0.80($p \leq 0.05$),7.00±1.22 ($p \leq 0.05$), 12.40±0.91 ($p \leq 0.05$) down fold, respectively, in large leaf compared to the small leaf, was also noted (Supplementary table 2). Thus, we concluded that differential expression of methyltransferases and demethylases likely rule the methylation at CATG sites in growing leaves.

RT-dependent quantitative PCR analysis was also performed to detect the expression level of these genes in mature leaves of transgenic control and virus infected plants. As expected, levels of three DNA methyltransferases, *SlDRM5*, *SlMET1*, and *SlCMT2*, were significantly decreased, 4.25±0.06 ($p \leq 0.05$), 2.19±0.20 ($p \leq 0.05$) and 2.82±0.14 ($p \leq 0.05$) fold, respectively in infection. Concurrently, transcript levels of two DNA demethylases, *SlDML1* and *SlDML2* were augmented in 2.03±0.84 ($p \leq 0.05$) and 3.15±0.79 ($p \leq 0.05$) folds, respectively in tested samples (Fig. 7B, Supplementary table 2). These observations suggest ToLCNDV infection inflicts both decreased methylation and enhanced demethylation for maintaining *SlTRN1* promoter as hypomethylated and fully active in all leaves.

3.7 Viral pathogenicity determinant protein AC4 is the major regulator of DNA demethylase

We have also designed experiments for identifying the viral factors causing misregulation of methylases and demethylases. Full length ORFs of replication initiation protein (AC1), replication enhancer protein (AC3) and pathogenicity determinant protein (AC4) were

agroinfiltrated in tomato leaves. Relative expression level of methylases and demethylases were determined by RT-dependent qPCR analysis on isolated RNA from infiltrated leaves. We observed *SlDRM5*, *SlMET1* and *SlCMT2* downregulation (1.16±0.03 fold, p≤ 0.05 and2.12±0.04 fold, p≤ 0.05, 2.08±0.15 fold, p≤ 0.05 respectively, in AC1; and 1.33±0.12 fold, p≤ 0.05 and 1.16±0.008 fold, p≤0.05, 1.60±0.055 fold, p≤0.05 respectively, in AC4) and *SlDML2* upregulation (3.44±0.90 fold, p≤ 0.05 and 3.28±0.21 fold, p≤ 0.05, respectively, in AC1 and AC4) in both AC1 and AC4 infiltration. Additionally, SlDML1 was significantly upregulated (2.28±0.06 fold, p≤ 0.05) in AC4 infiltrated leaf (Fig. 7C, and Supplementary Table 2). Not much change in gene expression pattern was seen upon AC3 infiltration. These observations are in line with our previous findings about expression pattern of methyltransferases and demethylases during infection. However, a closer inspection of the overall data suggests that the magnitude of upregulation of *SlDML2* during AC1 and AC4 infiltration was more compared to the changes noticed in other genes (Supplementary Table 2), thus, substantiating the pivotal role of the AC1 and AC4 proteins in *SlTRN1* promoter demethylation during infection.

3.8 Overexpression of DNA demethylase (SlDML2) restores hypomethylation of *SlTRN1* promoter and expression

To confirm the importance of demethylation and the stipulated role of demethylase in restoration of activity of the *SlTRN1* promoter, we investigated the effect of transient overexpression of a demethylase on TRN1-GUS expression in a large leaf. We have selected the DNA demethylase, *SlDML2* for this purpose, since its expression was abruptly changed in large leaves, during infection and AC1/AC4 infiltrations. The full length cDNA was amplified from tomato leaf total RNA, cloned in a binary vector (Fig. 8A, inset) and mobilized into Agrobacterium. The clone was Agroinfiltrated in multiple spots in large leaves for transient overexpression. Following two days of infiltration, DNA was isolated from the tissue and subjected to methylation sensitive PCR analysis. Non-amplification in PCR in *SlDML2* infiltrated and *Nla*III digested samples indicated methylations were absent; while higher band intensity in blank vector infiltrated leaves indicated existence of usual methylations at CATG sites (Fig. 8B). All controls were similar to the reactions described in previous sections.

Next, we investigated the effect of *SlDML2* expression on promoter activation. Histochemical GUS staining of the infiltrated leaves was performed. Intense blue coloration of *SlDML2*-

infiltrated leaves compared to only vector infiltrated samples confirmed re-activation of the promoter (Fig. 8D). Further, similar experiments with varied sizes of leaves were also carried out and GUS reporter activity was quantified by MUG-assays. Significant higher reporter activity in all categories of leaves was apparent (Fig. 8C), while maximum activation occurred in larger leaves. The intensity of increase was in the order of 2.68±0.13 ($p \leq 0.05$), 2.93±0.26 ($p \leq 0.05$) and 3.75±0.28 ($p \leq 0.05$) in small, medium and large leaves, respectively. These data strongly support that demethylation of SlTRN1 promoter via activation of demethylase keeps the promoter activated and restores promoter activity in older mature leaves.

Altogether, we have presented in vivo data reaffirming our previous observation of augmentation of vascular tissue specific expression of *TORNADO1* gene in tomato during ToLCNDV infection. Interestingly, expression of *SlTRN1* remains unabated in mature leaf during infection, which otherwise becomes transcriptionally silenced. Methylation at specific sequences of the promoter found to be the primary determinant for suppressing the gene expression in growing leaf, however, ToLCNDV infection interferes with the plant DNA methylation maintenance machinery to subdue the transcriptional gene silencing for reactivation of the gene.

Discussion:

Leaf development is a dynamic process involving multiple gene regulatory pathways that orchestrate the differentiation of component cells. In this study we dealt with a developmentally regulated gene, *SlTRN1*, playing a pivotal role in leaf symmetry and venation pattern formation, and lateral growth (Cnops et al. 2006). Previously, mostly via transient expression analyses, we had analyzed the mechanism of upregulation of the *SlTRN1* gene in tomato plant during ToLCNDV infection (Mandal et al. 2015). The importance of the *TRN1* gene insisted we delve into the mechanism of its regulation in vivo during ToLCNDV infection. One of the efficient methods of studying a gene's regulation without affecting the normal function of the gene is to utilize a promoter-reporter transgenic, thus, we had proceeded to generate such plant. Results presented here represent cumulative data obtained from the analysis of multiple transgenic lines.

In Arabidopsis, studies with mutant plants showed that the *TRN1* gene plays important role in the formation of procambium by sensing auxin canalization signal or participating in auxin transport regulation. *trn1* mutants had defective lamina symmetry, growth, and anomalous venation

patterning, perhaps due to defects in auxin signal sensing (Cnops et al. 2006). Histochemical staining of transverse sections of vegetative and reproductive organs of *SlTRN1* promoter transgenic plants also confirmed the limitation of TRN1 expression in vascular tissues (Figs. 1E-G and 2) indicating spatial expression pattern of *TRN1* is conserved. Another interesting observation was the temporal regulation of the *SlTRN1* gene expression in leaves of different growth stages, and ToLCNDV infected plants. We found weakened promoter activity with the progression of leaf growth (Fig. 3E-F). This observation indicated *SlTRN1* being a developmentally regulated gene, its expression was essential in the growing tissues or the younger parts and dispensable in the fully expanded and developed regions. The phenomenon is not related to transgene suppression since similar oppression of endogenous *SlTRN1* expression has also been noticed (Supplementary Fig. 2A). Also, multiple lines exhibited the same pattern of *SlTRN1* regulation, proving suppression of expression is transgene context-independent. In line with the previous studies from this laboratory, higher *SlTRN1* gene expression in ToLCNDV infected transgenic plant leaves (Mandal et al. 2015) has been confirmed by quantitative real-time PCR analysis, fluorometric MUG Assay and histochemical GUS staining experiments (Fig. 3C-G, 4A). Restoration of *SlTRN1* expression in mature leaves upon infection (Fig. 3E) was the most significant observation, which is supported by the fact that the degree of augmentation of promoter activity upon virus infection was higher in mature leaves compared to that of in the small leaves (Fig 3F, 3.49 compared to 2.6 fold, control vs. infected in large and small leaves). Thus, we can safely infer that the virus infection can reverse the effect of silencing of *SlTRN1* gene expression in mature leaves. WRKY16 transcription factor could readily induce expression of TRN1-GUS, similar to our previous transient assays (Mandal et al. 2015). However, the effect of WRKY16 seems to be independent of virus infection, since an equivalent amount of augmented activity was noticed in uninfected and infected leaves (Fig. 4B-D).

Epigenetic marking is one of the stable genomic modifications for silencing a gene whose function may not be immediately required. However, plants have developed mechanisms for flexible modifications including the requirement for continuous maintenance of localized cytosine methylation. In line, dynamic methylation of genic regions is associated with development and stress response in plants. During development, the pattern of DNA methylation in the genome changes as a result of a dynamic process involving both *de novo* DNA methylation and demethylation. As a consequence, differentiated cells develop a stable and

609 unique DNA methylation pattern that affects gene transcription in a tissue-specific manner. The
610 distinctive expression pattern of the *SlTRN1* gene in transgenic plants in developmental stages
611 and also during ToLCNDV infection tempted us to ponder on whether promoter-methylation
612 played an important role in regulating the gene expression. Methylation sensitive PCR analyses
613 indeed showed that (i) *SlTRN1* proximal promoter region is subjected to CATG (CHH)
614 methylations at multiple sites, (ii) more number of cells in large leaves harbour methylation in
615 these sites compared to the small leaves, (iii) promoter activity is negatively correlated to leaf
616 growth and methylation intensity, and (iv) almost absence of methylation marks in all sites tested
617 as well as restoration of promoter activity in mature leaves are correlated to ToLCNDV infection
618 (Fig. 5C and 3E). We have used a methylation blocker and proved that the variations in the
619 amplicon band intensities are the results of changed methylations, and showed restoration of
620 promoter activity. Thus *SlTRN1* promoter is repressed by CATG methylations (Fig. 6). Increased
621 methylation is not due to tissue culture or the context of integration of the transgene because wild
622 type plants and different transgenic lines exhibited similar pattern (Supplementary Fig3A). In
623 fact, A1 and A2 amplicons, harbouring two and one CATG sites, respectively, should be
624 amplified only from the endogenous genic region (Fig5A), while A3 and A4 amplicons,
625 harbouring one CATG site each, could be amplified from both endogenous and transgenes.
626 Hence, the results truly represent *SlTRN1* methylation status found in a wild type plant. Studies
627 with maize leaf showed that maintenance methylases are abundant in dividing tissues and
628 differential methylation pattern, mostly in the 5'and 3' ends of genes, was prominent between
629 cell division to cell expansion zones. Whereas, tissues with fully expanded cells had stabilized
630 methylation marks (Candaele et al. 2014). *SlTRN1* promoter methylation pattern (Fig. 5) is in
631 agreement with these previous studies.
632 Methylation is associated with the inactivation of gene transcription. In plants, the methylation
633 status is controlled by the dual action of methyltransferases and DNA demethylases along with
634 some methyl donors. Current knowledge suggests de novo DNA methylation in plants, as
635 observed in mature leaves, is RdDM (RNA-directed DNA methylation) dependent, and DRM2 is
636 essential for maintaining CHH methylation at the region of RdDM complex assembly. Active
637 DNA demethylation involves 5-mC DNA glycosylases. Among these ROS1, DML2 and DML3
638 are found in somatic cells. Our analysis of steady-state expression level of methyltransferases
639 and demethylases revealed 3 methyltransferases being significantly overexpressed in large leaves

with a concomitant decrease in the expression level of the three demethylases (Fig. 7A and Supplementary Table 2). Similar reports of upregulation in the level of four methyltransferases, *Smel*MET1, *Smel*CMT2, *Smel*CMT3a and *Smel*DRM3 in *Solanum melongena* during fruit development was observed, displaying augmented methylation is found at times during plant maturity (Moglia et al. 2019).Therefore, levels of expression of methylation and demethylation-related genes observed in our study agrees with the previous observations and methylation dynamics regulate the expression pattern of *SlTRN1* in small and large leaves.

We have shown previously that WRKY16 interaction with *SlTRN1* promoter region results in activated transcription. Two W-boxes are present midway between two *Nla*III sites which are 150 nucleotides distant (A1 amplicon, and Supplementary Fig. 1A), so may be CATG methylation (*Nla*III site) is not hindering WRKY binding, but overall promoter DNA methylation may preclude WRKY from binding in the promoter of the *SlTRN1* gene.

Arabidopsis plants having mutations in cytosine methylation machinery showed differential expression of pathogenesis-related genes. CHH methylation pattern is also dependent on pathogen types. An earlier report showed Viroids induce hypomethylation of the promoter region of rRNA genes resulting in increased expression (Martinez et al. 2014). Seemingly, a direct link exists between pathogenesis and the level of DNA methylation. Since *SlTRN1* activity is restored in mature leaves after ToLCNDV infection, we questioned whether the virus is meddling with the methyl cycle during infection by lessening or enhancement of some of the key regulatory enzymes that help to sustain methylation in mature leaves. Infection with ToLCNDV in the transgenic plants reduced the expression level of key maintenance and also *de novo* DNA methyltransferases with concurrent upregulation in transcript levels of two DNA demethylases in tested samples (Fig. 7B, Supplementary Table 2), essentially reversing methyl cycle gene expression levels in mature leaves. However, unlike the observations with mutant MET1 plants (Yang et al. 2019) we have detected hypomethylation of CHH sites in virus-infected leaves when MET1 was downregulated. Thus, the major reason for the hypomethylation phenomenon observed here may be attributed to the upregulation of demethylases.

Activation of the host DNA methylation pathway to methylate the virus genome to suppress its expression is a crucial defense strategy, while a virus recruits its proteins to counter the methylation pathways. Incidentally, the methylation status of several host genes is also compromised during an active infection. Proteomics studies of geminivirus infected plants

followed by VIGS-mediated specific gene silencing and infection analyses confirmed the role of RNA-directed DNA methylation (RdDM) pathway in host defense against the virus (Zhong et al. 2017; Zhang et al. 2011). On the other hand, several reports confirmed viral proteins as suppressors (VSRs) of RdDM. The C4 protein is capable of suppressing TGS and/or PTGS by, (i) inhibiting cell to spread of RNAi (Li et al. 2020), (ii) its interaction and inhibition of the enzymatic activity of methyl cycle core component S-adenosyl methionine synthetase (SAMS)(Ismayil et al. 2018), and (iii) inhibiting the function of Domains rearranged methyltransferase 2 (DRM2) to suppress methylation of the viral genome (Mei et al. 2020). AC4 of ToLCNDV (Vinutha et al. 2018) or V2 protein of TYLCV (Wang et al. 2020) inhibits AGO4 binding to viral DNA and methylation of the viral genome. V2-AGO4 complex readily localizes into Cajal body, thus might interfere with methylation of other genes. V2 protein of TYLCV also suppresses TGS by competitive inhibition of histone deacetylase 6 interaction with methyltransferase 1 (MET1) (Wang et al. 2018). Transgenic expression of Tomato leaf curl Taiwan virus (ToLCTWV) C2 protein in *N. banthamiana* dampened the level of a chromomethylase, due to reduced promoter activity. Hence, we intended to investigate which viral factors responsible for causing the changed regulations in the level of methyltransferases and/or DNA demethylases. Expectedly, ectopic expressions of AC1 and AC4 misregulated methyltransferases as well as DNA demethylases (Fig. 7B, Supplementary Table 2). However, only AC4 could somewhat mimic viral infection in terms of regulation of the methyl cycle enzymes (Supplementary Table 2).

Collectively, among the methyl cycle enzymes SlDML2 seemed to be the major mediator of infection-dependent reversible methylation of *SlTRN1* promoter due to its abrupt changes in expressions in mature leaves, by ToLCNDV infection, AC1 as well as AC4 infiltrations (Supplementary Table 2). Consequently, by transient infiltration assays, we found SlDML2 overexpression creates hypomethylation of the *SlTRN1* promoter in fully grown leaves and refurbishes promoter activity in all leaves. These data conclusively prove that demethylation of promoter via activation of a demethylase during ToLCNDV infection reactivates, otherwise transcriptionally suppressed, *SlTRN1* gene and restores expression in fully grown leaves.

A search in the tomato epigenome database (http://ted.bti.cornell.edu/cgi-bin/epigenome/home.cgi) of methylation pattern of *SlTRN1* genomic region revealed that 5kb up or downstream of the gene is rich in repeats, including MITE sequences. These repeat regions

are found to be highly methylated in fruits and chilling methylome. sRNAs are also seemed to be enriched for the repeat sequences. However, silencing of *SlTRN1* may not be linked to the adjacent repeat or transposable sequence silencing because we have also noticed the phenomenon in promoter transgene in multiple transgenic lines. Although small RNAs were not matched to the region proximal to the transcription start sites, the proximal promoter region in the leaf undergoes localized cytosine methylation at CG, CHH, CHG sites at specific regions. This is also raising the possibility that reversible methylations occur at additional sites which have not been analyzed yet.

The TGS and RdDM pathways have long been implicated in leaf curl disease severity. Transgenic expression of RNA-dependent RNA polymerase1 in *N. benthamiana* caused reduced susceptibility towards Tomato leaf curl Gujarat virus (ToLCGV) infection (Prakash et al. 2020). C4-mediated suppression of SAMS activity facilitated viral multiplication and determined symptom intensity (Ismayil et al. 2018). The C4 protein of tomato leaf curl Yunnan virus interacts with DRM2 to suppress methylation of the viral genome and a virus with a mutation in the C4 DRM2 interaction region produced only milder symptoms (Mei et al. 2020). C4 also indirectly inflicts accumulation of CyclinD1.1 in *N. benthamiana* plant causing abnormal cell division (Mei et al. 2018). AC4 protein disrupts the auxin biosynthesis/signalling pathway, vis-a-vis viral infection upregulates miR167 and miR393, further affecting auxin signalling in leaf. Besides, exogenous auxin application somewhat ameliorates disease symptoms, signifying suppression of auxin signalling is linked to typical symptom manifestation (Vinutha et al. 2020). Auxin canalization is one of the important factors in vein development and TRN1 protein involved in sensing canalization signal and vein reticulation. Enhanced or ectopic expression of auxin signaling genes leads to leaf developmental defect. The phenotype of PINOID, enhancer of polar auxin transport, overexpressing plants resembled that of auxin transport or sensitivity mutants (Saini et al. 2017) including stunted rosette formation. Overexpression of SlTIR1 results in abnormal leaf development having a smaller leaf length to width ratio in tomato (Ren et al. 2011). Thus, it is likely that the ectopic expression of *SlTRN1* due to ToLCNDV infection contributes to typical leaf curl symptom manifestation.

Figure legends

Fig.1. GUS gene expression pattern in SlTRN1-GUS transgenic tomato plants. A, Photograph of about one month old control and transgenic TRN1-GUS tomato plants. B, GUS-stained images of control and transgenic leaf, stem, root, and twig (C). D, Relative level of GUS activity in different organs of control and transgenic plant. E, Histochemical localization of GUS expression in transverse sections of leaf, stem (F) and longitudinal section of transgenic stem (G). *, significant change.

Fig. 2. GUS gene expression pattern in reproductive organs of SlTRN1-GUS plants. Photographs showing GUS stained control tomato flower (A), transgenic bud (B), flower (C), calyx (D), androecium (E), gynoecium (G) and receptacle, imaged after removal of chlorophyll.

Fig 3. *SlTRN1* promoter activity during ToLCNDV infection. A, Photographs of about one month old uninfected and virus infected SlTRN1-GUS transgenic tomato plants. B, Agarose gel photograph showing resolved products of viral coat protein and movement protein gene specific PCRs with genomic DNA of uninfected (lanes 1-3) and ToLCNDV infected (lanes 4-6) tomato plants. C, Data of MUG assay showing *SlTRN1* promoter activation upon ToLCNDV infection in different lines. D, GUS stained roots of transgenic uninfected and infected plants. E, GUS stained leaves of different growth stages from control, transgenic uninfected and transgenic infected plants. F, Quantitative assessment of *SlTRN1* promoter activation in different sized leaves upon ToLCNDV infection. G, Transverse section of GUS stained uninfected and infected transgenic leaf showing enhanced GUS staining in vascular elements. *, significant change.

Fig 4: Transcriptional activation of *SlTRN1* promoter during ToLCNDV infection and WRKY infiltration. A, Quantitative RT-PCR data showing GUS gene is highly overexpressed during TolCNDV infection in three lines tested. B, Relative expression level of GUS gene upon WRKY16 infiltration in transgenics. C, Regulation of promoter activity in two different sized leaves upon WRKY16 infiltration. D, Further upregulation of GUS gene expression upon transient expression of WRKY16 in ToLCNDV infected leaves. *, significant change.

762

763 Fig 5: Methylation status of *SlTRN1* promoter. A, Scheme depicting the promoter region, 730 nt
764 upstream of the ATG, of *SlTRN1*. Green bars indicating positions of *Nla*III recognition sites.
765 Forward primers, orange arrow, and reverse primers, blue arrow, used in methylation sensitive
766 PCRs are indicated. A1, A2, A3 and A4 are different PCR amplicons. TSS, Transcription start
767 site. B, Nucleotide sequence of *SlTRN1* promoter region, forward primers are marked in blue
768 font, reverse primers in orange font, and purple font represents the overlapping F4 and R3
769 primers. G in red font indicates the boundary of the promoter transgene in SlTRN1-GUS plants.
770 *Nla*III sites are highlighted with green. C, Agarose gel photograph of resolved methylation
771 sensitive PCR amplicons obtained with uninfected and virus infected transgenic plants.
772 Amplification from a genomic region with no *Nla*III cut sites used as loading control.

773

774 Fig 6: Promoter methylation and activity analyses after treatment with a methylation blocker. A,
775 Agarose gel photograph showing profile of methylation sensitive PCR amplicons in untreated
776 and 5-azacytidine treated transgenic plant leaves. Amplification profile from a genomic region
777 with no *Nla*III sites used as loading control. B, Promoter activity assay showing magnitude of
778 *SlTRN1* promoter reactivation upon treatment with 5-azacytidine in different sized leaves. C,
779 GUS staining of 5-azacytidine untreated and treated transgenic mature leaf. Intense staining upon
780 treatment also confirms *SlTRN1* promoter reactivation. *, significant change.

781

782 Fig 7: Expression level of four DNA methyltransferases and three DNA demethylases under
783 normal physiological condition and various treatments. Relative expression level of four DNA
784 methyltransferases and three DNA demethylases in varied sizes leaves (A), control and
785 ToLCNDV infected plants (B) and upon transient overexpression of ToLCNDV replication
786 initiation protein AC1, replication maintenance protein AC3 and pathogenicity determinant
787 protein AC4 (C). *, significant change.

788

789 Fig 8: Restoration of promoter activity by DNA demethylase in mature leaves. A, Agarose gel
790 photograph showing amplification and clone confirmation of *SlDML2* full length (Fl) CDS

(arrow). B, Agarose gel photograph showing resolved bands of methylation sensitive PCR amplicons in only vector and *SlDML2* infiltrated transgenic tomato leaves. Amplification of a genomic region with no *Nla*III sites used as loading control. C, MUG-assay data showing magnitude of *SlTRN1* promoter activation upon full length *SlDML2* infiltration in different sized leaves. D, GUS staining of vector and *SlDML2* infiltrated transgenic mature tomato leaves. Intense staining upon SlDML2 expression confirmed reactivation of *SlTRN1* promoter. *, significant change.

Supplementary Figure 1. Production of TRN1-GUS transgenic tomato plants and confirmation of gene integration. A, Construct used in transformation of tomato. Scheme of -344/+UTR cloned in pCAMBIA1304 vector, upstream of GUS gene, depicting the cis-elements present in the sequence. B, Different stages of transgenic development includes callus formation, shoot regeneration, root induction and entire plant formation from cotyledonary leaf explant by Agrobacteria-mediated transformation. C, Agarose gel photograph showing amplification of *hptII* gene from cDNA of five transgenic lines. The right gel picture shows amplicons from vector backbone specific primers. +Ve, positive control. D. Left panel, Agarose gel picture indicating quality of RNA used in the experiment; middle panel, relative expression level of GUS transcript in five transgenic lines. Inset, agarose gel photograph of resolved bands of semiquantitative PCR, showing amplification of GUS transcript from 5 lines; -RT, RT independent PCR; +Ve, positive control, and right panel, single melt peak confirmed amplification of only a major band.

Supplementary Figure 2. *SlTRN1* promoter activity assays in leaf growth, and upon NAC transcription factor infiltration or abiotic stress treatment. A, Relative expression pattern of SlTRN1 mRNA in different sized leaves of wild type plant, and inset, agarose gel photograph showing resolved bands of the RT-PCR. GUS activity in NAC3, 4 and 8 transcription factor (SolyC06g073050, SolyC03g078120 and SolyC07g066330, respectively) infiltration (B), and exposure of transgenic plants to abiotic stresses (C). Unaltered GUS activity in both experiments indicated minimum influence of these treatments on *SlTRN1* expression.

Supplementary Figure 3. Methylation sensitive PCR analysis with wild type plants, and an alternate methylation sensitive enzyme. A, left panel, Agarose gel photograph showing methylation sensitive PCR amplicons in wild type tomato plant with *Nla*III as methylation sensitive enzyme. The amplification pattern follows the trend as in TRN1-GUS transgenic tomato plant. A, right panel, bar graph showing quantification of methylation sensitive PCR amplicons in wild type tomato plant. B, Agarose gel photograph showing methylation sensitive PCR amplicons with *Dpn*I as the methylation sensitive enzyme. Equal intensity products were obtained due to the lack of *Dpn*I site in the promoter region. *, significant change as observed by ANOVA analysis.

Supplementary Figure 4. Bar graph showing quantification of methylation sensitive PCR amplicons in ToLCNDV infection (A), 5-Azacytidine treatment (B) and *SlDML2* infiltration (C). *, significant change as observed by ANOVA analysis.

Acknowledgement

This work is supported by DST, GoI, INSPIRE fellowship to SC and intramural funding of Bose Institute to PK. Authors are thankful to Professor Shubho Chaudhuri, Pratiti Dasgupta, members of Chaudhuri lab and the Central Instrument Facility of Bose Institute. Statistical analysis support from Dr. Sanat K. Das of Bose Institute is highly acknowledged. We thank Prof. Somnath Bhattacharyya, Bidhan Chandra Krishi Viswavidyalaya for assistance with plant physiological parameter analysis.

References:

Bartels A, Han Q, Nair P, Stacey L, Gaynier H, Mosley M, Huang QQ, Pearson JK, Hsieh T-F, An Y-QC, Xiao W (2018) Dynamic DNA Methylation in Plant Growth and Development. Int J Mol Sci 19 (7):2144. doi:10.3390/ijms19072144

Böhmdorfer G, Rowley MJ, Kuciński J, Zhu Y, Amies I, Wierzbicki AT (2014) RNA-directed DNA methylation requires stepwise binding of silencing factors to long non-coding RNA. The Plant Journal : for cell and molecular biology 79 (2):181-191. doi:10.1111/tpj.12563

852 Buchmann RC, Asad S, Wolf JN, Mohannath G, Bisaro DM (2009) Geminivirus AL2 and L2 Proteins
853 Suppress Transcriptional Gene Silencing and Cause Genome-Wide Reductions in Cytosine
854 Methylation. Journal of virology 83 (10):5005-5013. doi:doi:10.1128/JVI.01771-08
855 Candaele J, Demuynck K, Mosoti D, Beemster GTS, Inzé D, Nelissen H (2014) Differential Methylation
856 during Maize Leaf Growth Targets Developmentally Regulated Genes Plant Physiology 164
857 (3):1350-1364. doi:10.1104/pp.113.233312
858 Cnops G, Neyt P, Raes J, Petrarulo M, Nelissen H, Malenica N, Luschnig C, Tietz O, Ditengou F, Palme K,
859 Azmi A, Prinsen E, Van Lijsebettens M (2006) The TORNADO1 and TORNADO2 genes function in
860 several patterning processes during early leaf development in Arabidopsis thaliana. Plant Cell 18
861 (4):852-866. doi:10.1105/tpc.105.040568
862 Dasgupta P, Chaudhuri S (2019) Analysis of DNA Methylation Profile in Plants by Chop-PCR. In:
863 Gassmann W (ed) Plant Innate Immunity: Methods and Protocols. Springer New York, New York,
864 NY, pp 79-90. doi:10.1007/978-1-4939-9458-8_9
865 Díaz-Pendón JA, Ding SW (2008) Direct and indirect roles of viral suppressors of RNA silencing in
866 pathogenesis. Annual review of phytopathology 46:303-326.
867 doi:10.1146/annurev.phyto.46.081407.104746
868 Ding S-W (2010) RNA-based antiviral immunity. Nature Reviews Immunology 10 (9):632-644.
869 doi:10.1038/nri2824
870 Elbashir SM, Martinez J, Patkaniowska A, Lendeckel W, Tuschl T (2001) Functional anatomy of siRNAs for
871 mediating efficient RNAi in Drosophila melanogaster embryo lysate. EMBO J 20 (23):6877-6888.
872 doi:10.1093/emboj/20.23.6877
873 Gorovits R, Moshe A, Amrani L, Kleinberger R, Anfoka G, Czosnek H (2017) The six Tomato yellow leaf
874 curl virus genes expressed individually in tomato induce different levels of plant stress response
875 attenuation. Cell Stress Chaperones 22 (3):345-355. doi:10.1007/s12192-017-0766-0
876 Guzmán-Benito I, Donaire L, Amorim-Silva V, Vallarino JG, Esteban A, Wierzbicki AT, Ruiz-Ferrer V, Llave
877 C (2019) The immune repressor BIR1 contributes to antiviral defense and undergoes
878 transcriptional and post-transcriptional regulation during viral infections. New Phytol 224
879 (1):421-438. doi:10.1111/nph.15931
880 Ismayil A, Haxim Y, Wang Y, Li H, Qian L, Han T, Chen T, Jia Q, Yihao Liu A, Zhu S, Deng H, Gorovits R,
881 Hong Y, Hanley-Bowdoin L, Liu Y (2018) Cotton Leaf Curl Multan virus C4 protein suppresses
882 both transcriptional and post-transcriptional gene silencing by interacting with SAM synthetase.
883 PLOS Pathogens 14 (8):e1007282. doi:10.1371/journal.ppat.1007282
884 Li W, Liu H, Cheng ZJ, Su YH, Han HN, Zhang Y, Zhang XS (2011) DNA methylation and histone
885 modifications regulate de novo shoot regeneration in Arabidopsis by modulating WUSCHEL
886 expression and auxin signaling. PLoS Genet 7 (8):e1002243-e1002243.
887 doi:10.1371/journal.pgen.1002243
888 Li Z, Du Z, Tang Y, She X, Wang X, Zhu Y, Yu L, Lan G, He Z (2020) C4, the Pathogenic Determinant of
889 Tomato Leaf Curl Guangdong Virus, May Suppress Post-transcriptional Gene Silencing by
890 Interacting With BAM1 Protein. Frontiers in Microbiology 11 (851).
891 doi:10.3389/fmicb.2020.00851
892 Liu H, Zhang H, Dong YX, Hao YJ, Zhang XS (2018) DNA METHYLTRANSFERASE1-mediated shoot
893 regeneration is regulated by cytokinin-induced cell cycle in Arabidopsis. New Phytologist 217
894 (1):219-232. doi:https://doi.org/10.1111/nph.14814
895 Llave C (2010) Virus-derived small interfering RNAs at the core of plant-virus interactions. Trends in
896 plant science 15 (12):701-707. doi:10.1016/j.tplants.2010.09.001
897 Luna AP, Rodríguez-Negrete EA, Morilla G, Wang L, Lozano-Durán R, Castillo AG, Bejarano ER (2017) V2
898 from a curtovirus is a suppressor of post-transcriptional gene silencing. Journal of General
899 Virology 98 (10):2607-2614. doi:https://doi.org/10.1099/jgv.0.000933

Mandal A, Sarkar D, Kundu S, Kundu P (2015) Mechanism of regulation of tomato TRN1 gene expression in late infection with tomato leaf curl New Delhi virus (ToLCNDV). Plant Sci 241:221-237. doi:10.1016/j.plantsci.2015.10.008

Martinez G, Castellano M, Tortosa M, Pallas V, Gomez G (2014) A pathogenic non-coding RNA induces changes in dynamic DNA methylation of ribosomal RNA genes in host plants. Nucleic Acids Research 42 (3):1553-1562. doi:10.1093/nar/gkt968

Mei Y, Wang Y, Li F, Zhou X (2020) The C4 protein encoded by tomato leaf curl Yunnan virus reverses transcriptional gene silencing by interacting with NbDRM2 and impairing its DNA-binding ability. PLOS Pathogens 16 (10):e1008829. doi:10.1371/journal.ppat.1008829

Mei Y, Yang X, Huang C, Zhang X, Zhou X (2018) Tomato leaf curl Yunnan virus-encoded C4 induces cell division through enhancing stability of Cyclin D 1.1 via impairing NbSKη -mediated phosphorylation in Nicotiana benthamiana. PLoS pathogens 14 (1):e1006789. doi:10.1371/journal.ppat.1006789

Moglia A, Gianoglio S, Acquadro A, Valentino D, Milani AM, Lanteri S, Comino C (2019) Identification of DNA methyltransferases and demethylases in Solanum melongena L., and their transcription dynamics during fruit development and after salt and drought stresses. PLOS ONE 14 (10):e0223581. doi:10.1371/journal.pone.0223581

Prakash V, Singh A, Singh AK, Dalmay T, Chakraborty S (2020) Tobacco RNA-dependent RNA polymerase 1 affects the expression of defence-related genes in Nicotiana benthamiana upon Tomato leaf curl Gujarat virus infection. Planta 252 (1):11. doi:10.1007/s00425-020-03417-y

Raja P, Sanville BC, Buchmann RC, Bisaro DM (2008) Viral genome methylation as an epigenetic defense against geminiviruses. Journal of virology 82 (18):8997-9007. doi:10.1128/JVI.00719-08

Ren Z, Li Z, Miao Q, Yang Y, Deng W, Hao Y (2011) The auxin receptor homologue in Solanum lycopersicum stimulates tomato fruit set and leaf morphogenesis. Journal of Experimental Botany 62 (8):2815-2826. doi:10.1093/jxb/erq455

Rodríguez-Negrete E, Lozano-Durán R, Piedra-Aguilera A, Cruzado L, Bejarano ER, Castillo AG (2013) Geminivirus Rep protein interferes with the plant DNA methylation machinery and suppresses transcriptional gene silencing. New Phytologist 199 (2):464-475. doi:https://doi.org/10.1111/nph.12286

Ruiz-Ferrer V, Voinnet O (2009) Roles of Plant Small RNAs in Biotic Stress Responses. Annual review of plant biology 60:485-510. doi:10.1146/annurev.arplant.043008.092111

Saini K, Markakis MN, Zdanio M, Balcerowicz DM, Beeckman T, De Veylder L, Prinsen E, Beemster GTS, Vissenberg K (2017) Alteration in Auxin Homeostasis and Signaling by Overexpression Of PINOID Kinase Causes Leaf Growth Defects in Arabidopsis thaliana. Frontiers in Plant Science 8 (1009). doi:10.3389/fpls.2017.01009

Vanitharani R, Chellappan P, Pita JS, Fauquet CM (2004) Differential roles of AC2 and AC4 of cassava geminiviruses in mediating synergism and suppression of posttranscriptional gene silencing. Journal of virology 78 (17):9487-9498. doi:10.1128/jvi.78.17.9487-9498.2004

Vinutha T, Kumar G, Garg V, Canto T, Palukaitis P, Ramesh SV, Praveen S (2018) Tomato geminivirus encoded RNAi suppressor protein, AC4 interacts with host AGO4 and precludes viral DNA methylation. Gene 678:184-195. doi:https://doi.org/10.1016/j.gene.2018.08.009

Vinutha T, Vanchinathan S, Bansal N, Kumar G, Permar V, Watts A, Ramesh SV, Praveen S (2020) Tomato auxin biosynthesis/signaling is reprogrammed by the geminivirus to enhance its pathogenicity. Planta 252 (4):51. doi:10.1007/s00425-020-03452-9

Wang B, Yang X, Wang Y, Xie Y, Zhou X (2018) Tomato Yellow Leaf Curl Virus V2 Interacts with Host Histone Deacetylase 6 To Suppress Methylation-Mediated Transcriptional Gene Silencing in Plants. Journal of virology 92 (18). doi:10.1128/jvi.00036-18

Wang H, Hao L, Shung C-Y, Sunter G, Bisaro DM (2003) Adenosine Kinase Is Inactivated by Geminivirus AL2 and L2 Proteins. The Plant Cell 15 (12):3020-3032. doi:10.1105/tpc.015180

Wang L, Ding Y, He L, Zhang G, Zhu JK, Lozano-Duran R (2020) A virus-encoded protein suppresses methylation of the viral genome through its interaction with AGO4 in the Cajal body. eLife 9. doi:10.7554/eLife.55542

Wang Y, Xue X, Zhu JK, Dong J (2016) Demethylation of ERECTA receptor genes by IBM1 histone demethylase affects stomatal development. Development (Cambridge, England) 143 (23):4452-4461. doi:10.1242/dev.129932

Yang J-Y, Iwasaki M, Machida C, Machida Y, Zhou X, Chua N-H (2008) βC1, the pathogenicity factor of TYLCCNV, interacts with AS1 to alter leaf development and suppress selective jasmonic acid responses. Genes & Development 22 (18):2564-2577. doi:10.1101/gad.1682208

Yang Y, Tang K, Datsenka TU, Liu W, Lv S, Lang Z, Wang X, Gao J, Wang W, Nie W, Chu Z, Zhang H, Handa AK, Zhu J-K, Zhang H (2019) Critical function of DNA methyltransferase 1 in tomato development and regulation of the DNA methylome and transcriptome. Journal of Integrative Plant Biology 61 (12):1224-1242. doi:https://doi.org/10.1111/jipb.12778

Zhang Z, Chen H, Huang X, Xia R, Zhao Q, Lai J, Teng K, Li Y, Liang L, Du Q, Zhou X, Guo H, Xie Q (2011) BSCTV C2 Attenuates the Degradation of SAMDC1 to Suppress DNA Methylation-Mediated Gene Silencing in Arabidopsis The Plant Cell 23 (1):273-288. doi:10.1105/tpc.110.081695

Zhong X, Wang ZQ, Xiao R, Wang Y, Xie Y, Zhou X (2017) iTRAQ analysis of the tobacco leaf proteome reveals that RNA-directed DNA methylation (RdDM) has important roles in defense against geminivirus-betasatellite infection. Journal of Proteomics 152:88-101. doi:https://doi.org/10.1016/j.jprot.2016.10.015

Figures

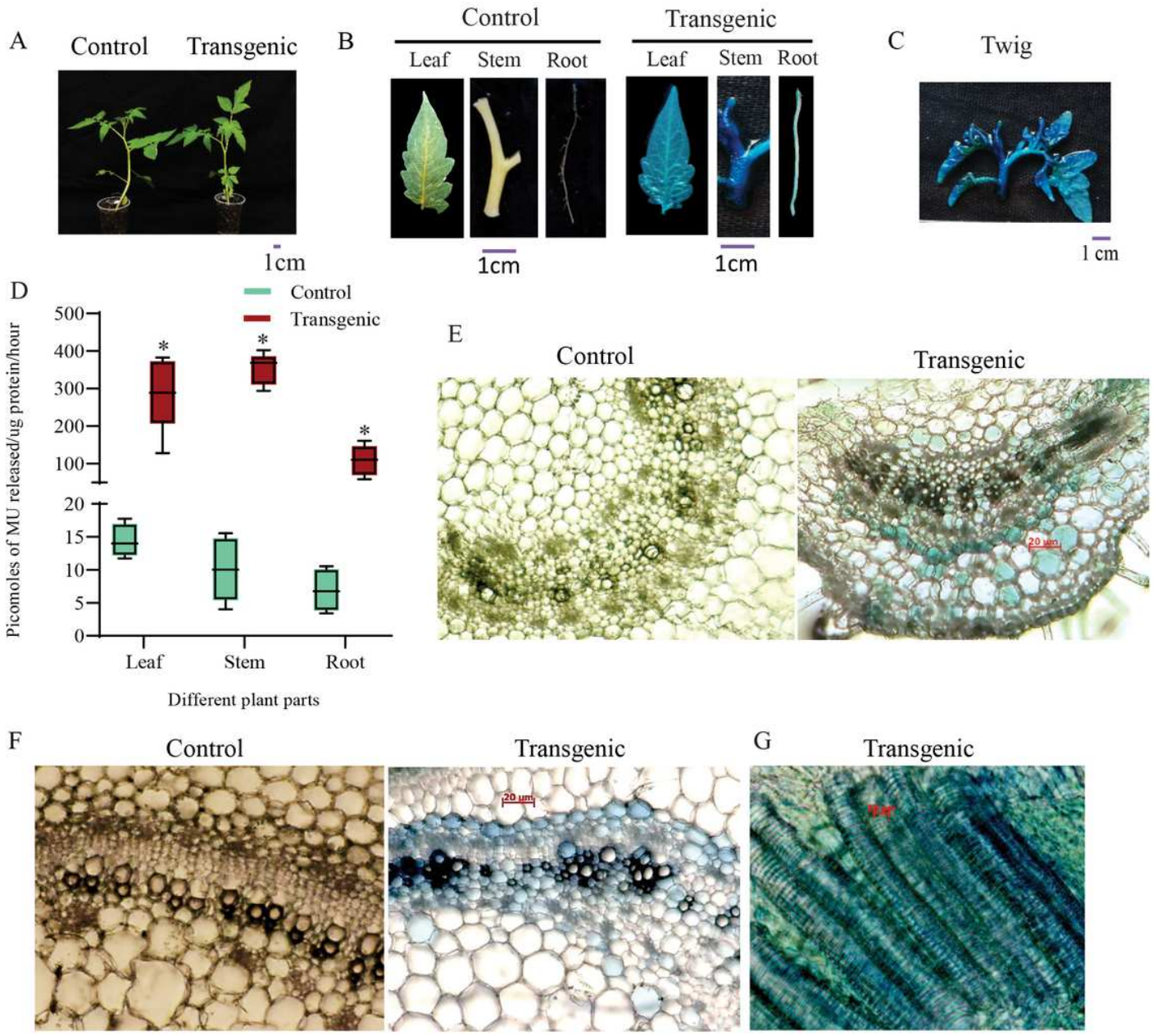

Figure 1

GUS gene expression pattern in SlTRN1-GUS transgenic tomato plant. A, Photograph of about one month old control and transgenic tomato plant. B, GUS stained images of control and transgenic leaf,stem,- root and twig(C). D, Relative level of GUS activity in different organs of control and transgenic plant. E, Histochemical localization of GUS expression in transverse sections of leaf,stem (F) and longitudinal section of transgenic stem (G). *, significant change.

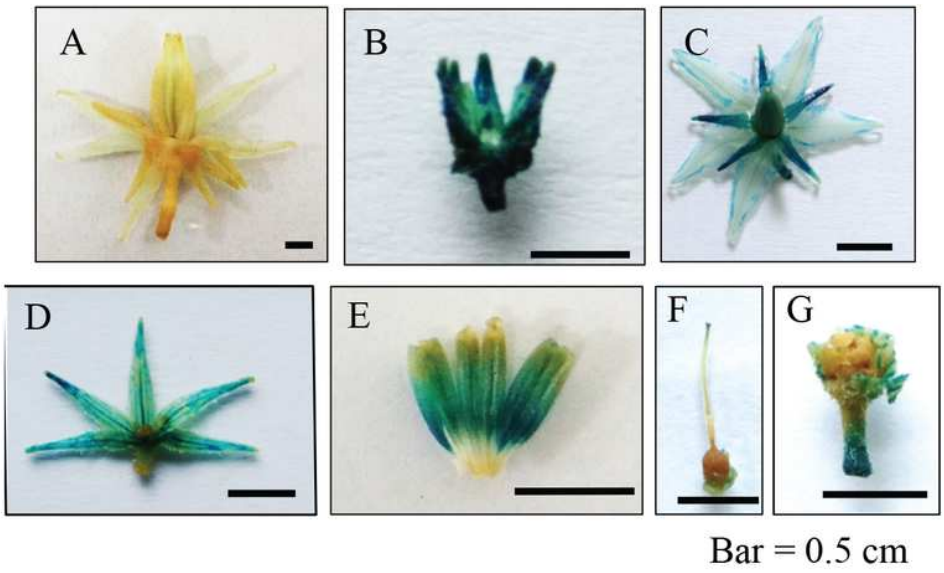

Figure 2

GUS gene expression pattern in reproductive organs of SlTRN1-GUS plants. Photographs of GUS stained control tomato flower (A), transgenic bud (B), flower (C), calyx (D), androecium (E), gynoecium (G) and receptacle , imaged after removal of chlorophyll.

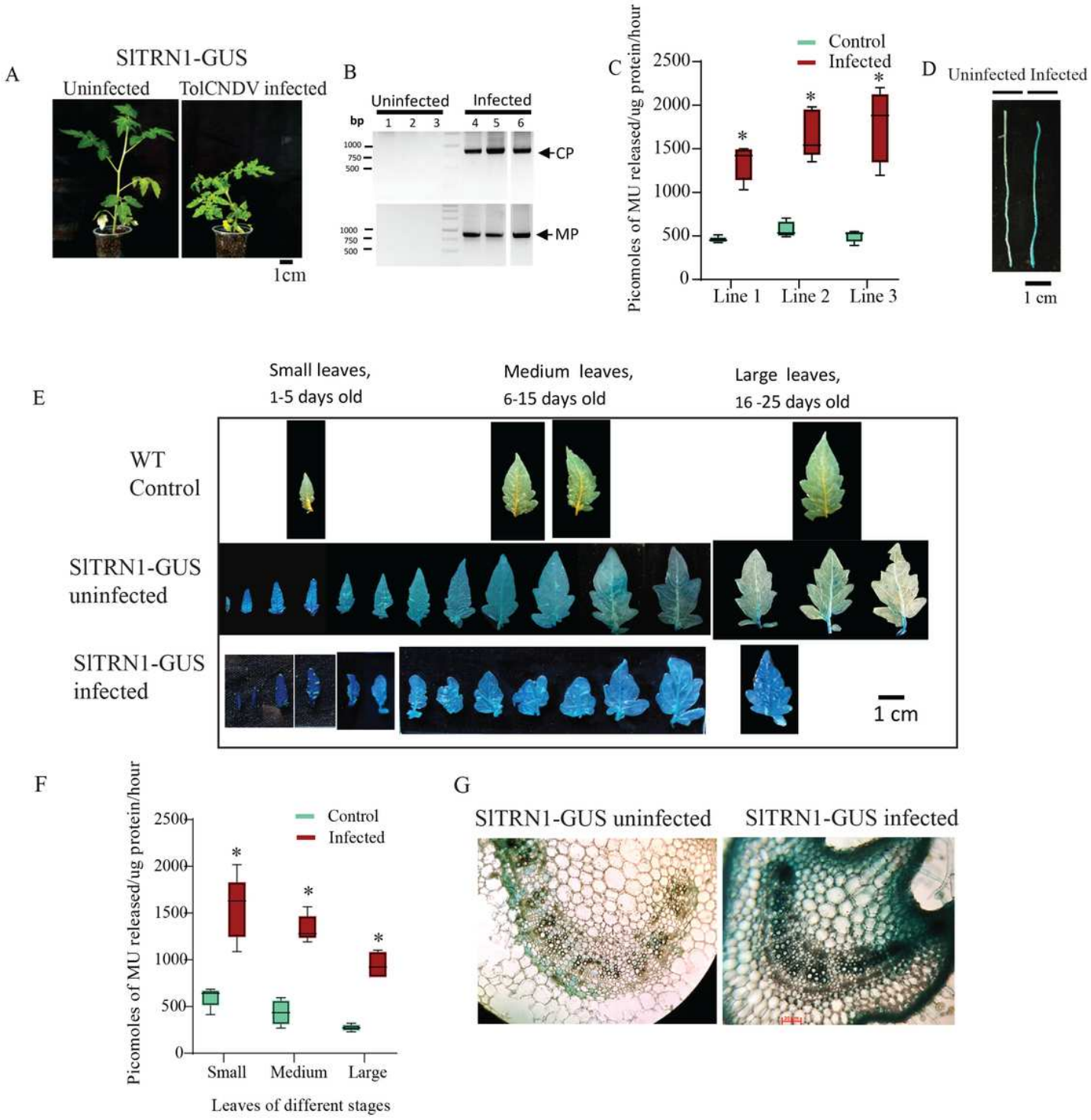

Figure 3

SlTRN1 promoter activity during TolCNDV infection. A, Photographs of about one month old uninfected and virus infected SlTRN1-GUS transgenic tomato plants. B, Agarose gel photograph showing resolved products of viral coat protein and movement protein gene specific PCRs with genomic DNA of uninfected (lanes 1-3) and TolCNDV infected (lanes 4-6) tomato plants. C, Data of MUG assay showing SlTRN1 promoter activation upon TolCNDV infection in different lines. D, GUS stained roots of transgenic uninfected and infected plants. E, GUS stained leaves of different growth stages from control, transgenic

uninfected and transgenic infected plants. F, Quantitative assessment of SlTRN1 promoter activation in different sized leaves upon TolCNDV infection. G, Transverse section of GUS stained uninfected and infected transgenic leaf showing enhanced GUS staining in vascular elements. *, significant change.

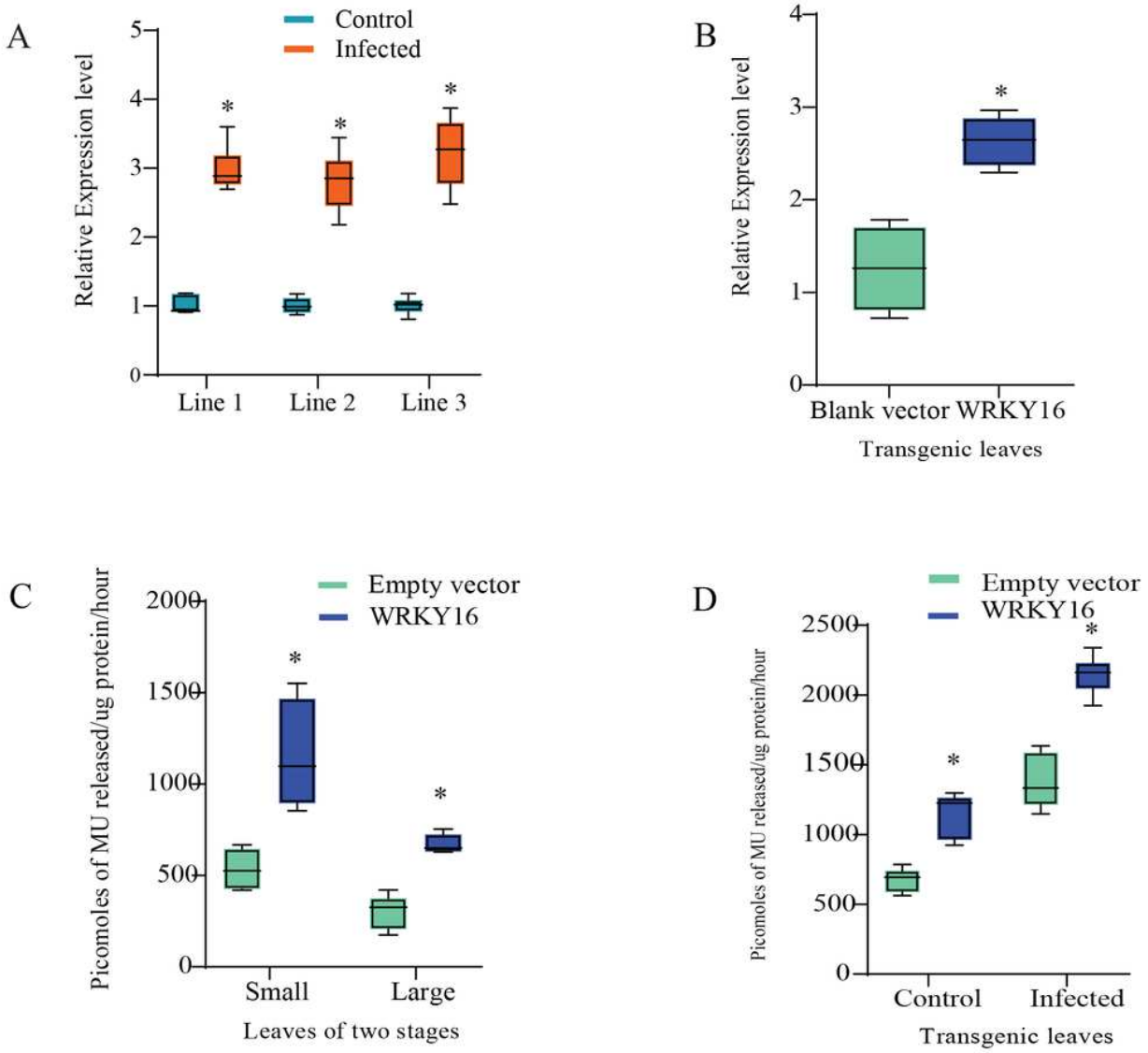

Figure 4

Transcriptional activation of SlTRN1 promoter during TolCNDV infection and WRKY infiltration . A, Quantitative RT-PCR data showing GUS gene is highly overexpressed during TolCNDV infection in three lines tested. B, Relative expression level of GUS gene upon WRKY16 infiltration in transgenics. C, Regulation of promoter activity in two different sized leaves upon WRKY16 infiltration. D, Further upregulation of GUS gene expression upon transient expression of WRKY16 in TolCNDV infected leaves. *,significant change.

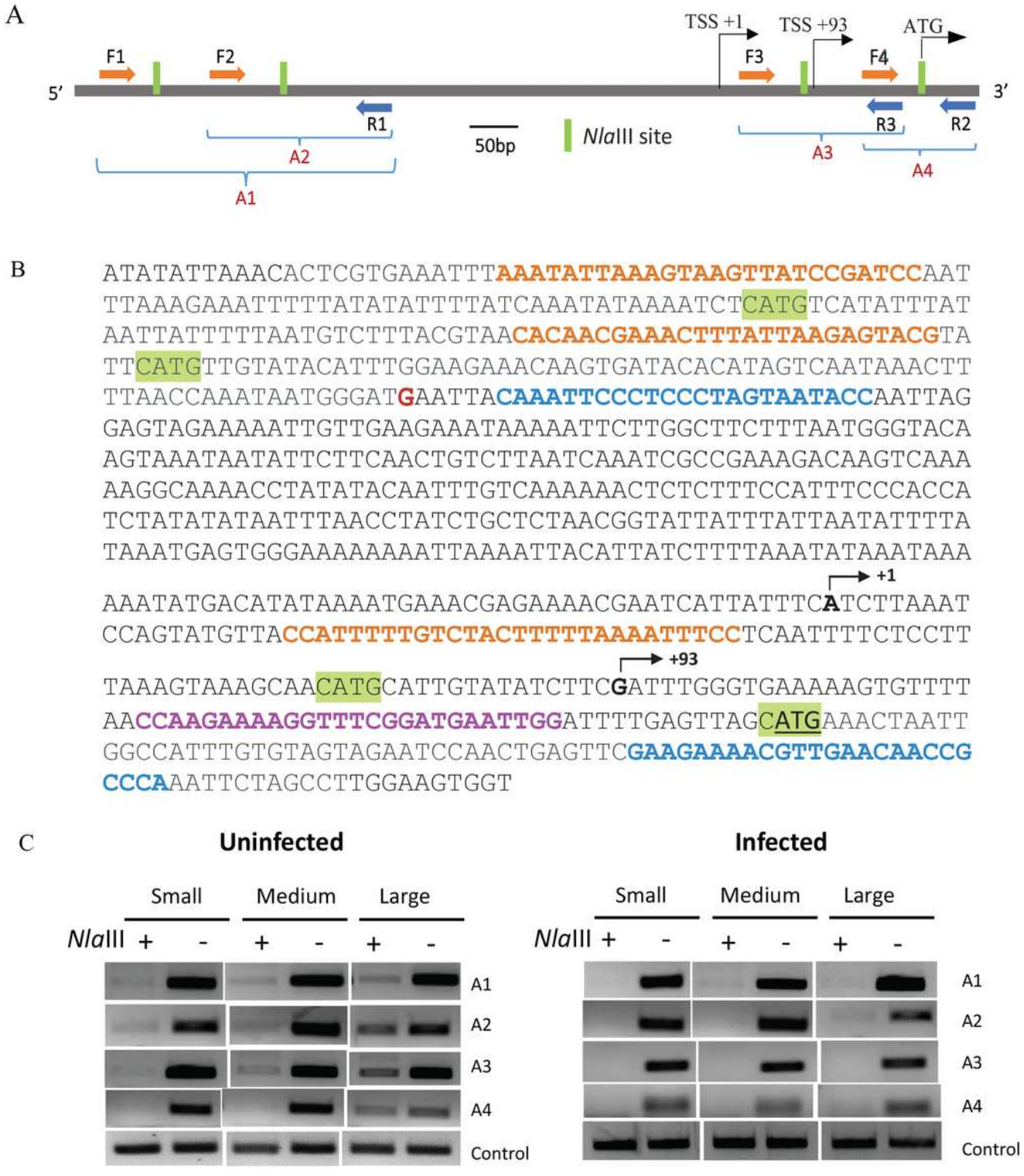

Figure 5

Methylation status of SlTRN1 promoter. A, Scheme depicting the promoter region,730 nt upstream of the ATG, of SlTRN1. Green bars indicating positions of NlaIII recognition sites. Forward primers, orrange arrow, and reverse primers, blue arrow, used in the methylation sensitive PCRs are indicated. A1, A2, A3, A4 are different PCR amplicons. TSS, Transcription start site. B, Nucleotide sequence of SlTRN1 promoter region, forward primers are marked in orange font, reverse primers in blue font, and purple font represents

the overlapping F4 and R3 primers. G in red font indicates the boundary of the promoter transgene in SlTRN1-GUS plants. NlaIII sites are highlighted with green. C, Agarose gel photograph of resolved methylation sensitive PCR amplicons obtained with uninfected and virus infected transgenic plants. Amplification from a genomic region with no NlaIII cut sites used as loading control.

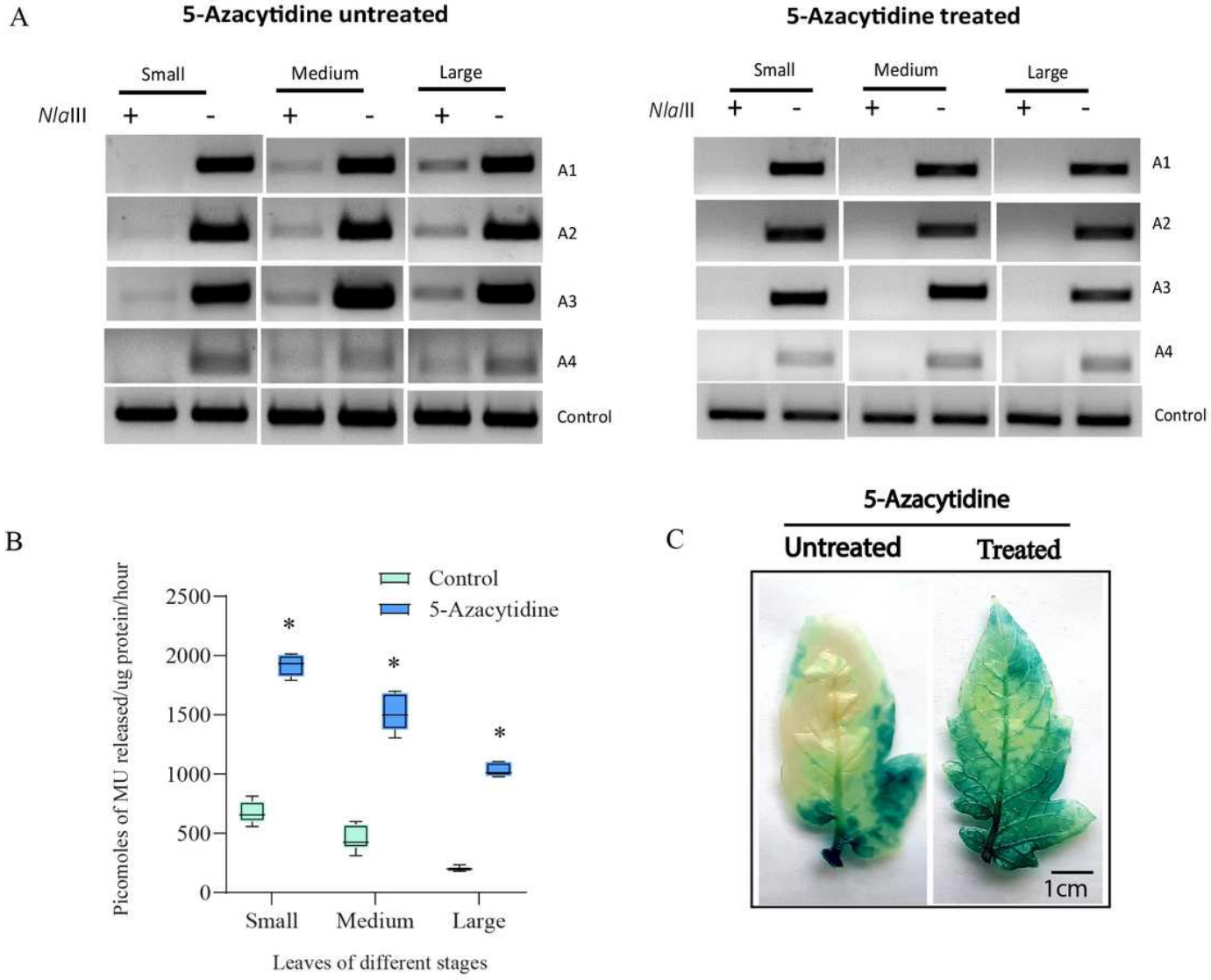

Figure 6

Promoter methylation and activity analyses after treatment with a methylation blocker . A, Agarose gel photograph showing profile of methylation sensitive PCR amplicons in untreated and 5-azacytidine treated transgenic plant leaves. Amplification profile from a genomic region with no NlaIII sites used as loading control. B, Promoter activity assay showing magnitude of SlTRN1 promoter reactivation upon treatement with 5-azacytidine in different sized leaves. C, GUS staining of 5-azacytidine untreated and treated mature leaf . Intense staining upon treatment also confirms SlTRN1 promoter reactivation. *,significant change.

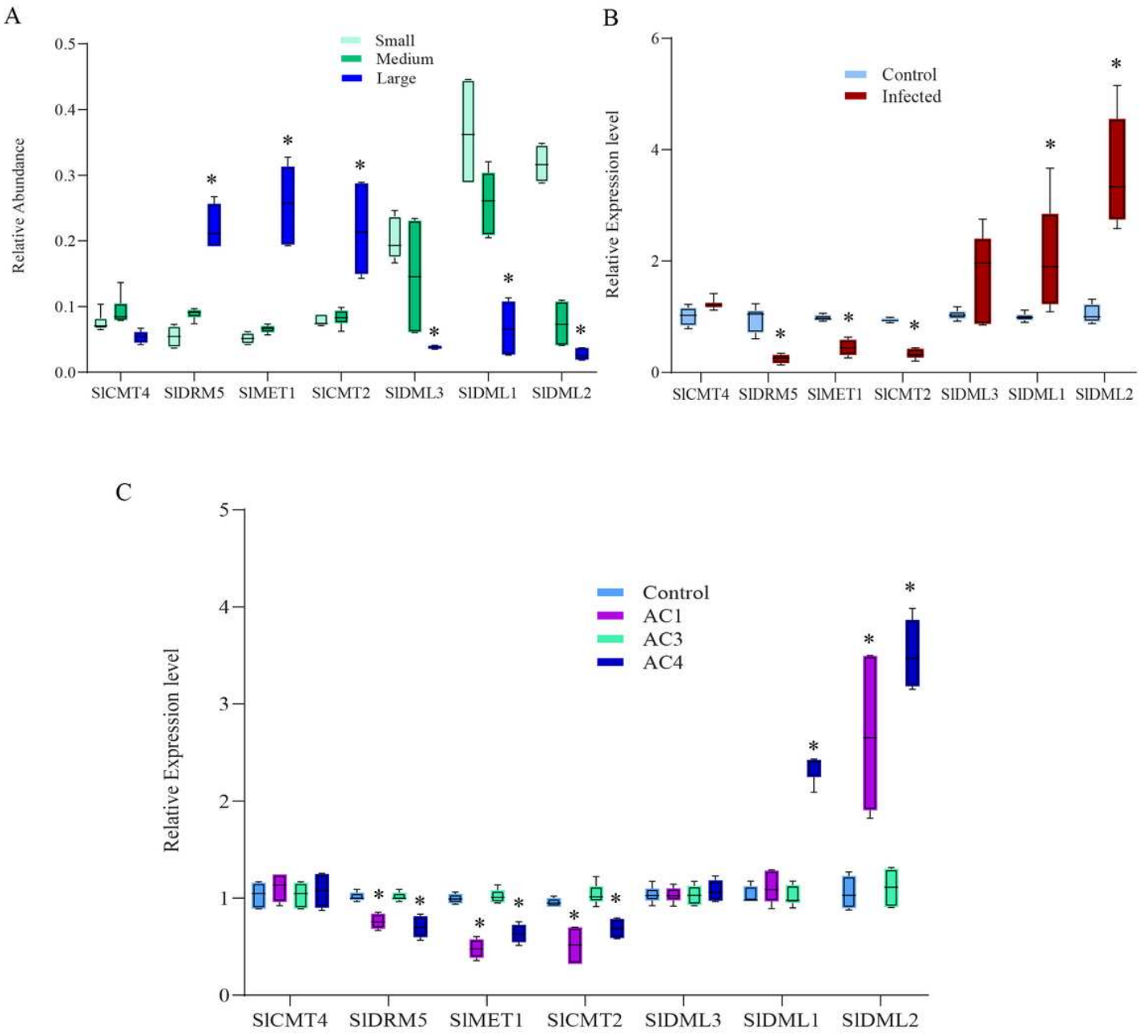

Figure 7

Expression level of four DNA methyltransferase and three DNA demethylases under normal physiological condition and various treatments..Relative expression level of four DNA methyltransferases and three DNA demethylases in varied size leaves (A), control and TolCNDV infected plants (B) and upon transient overexpression of TolCNDV replication initiation protein AC1, replication maintenance protein AC3 and pathogenecity determinant protein AC4 (C).*,significant change.

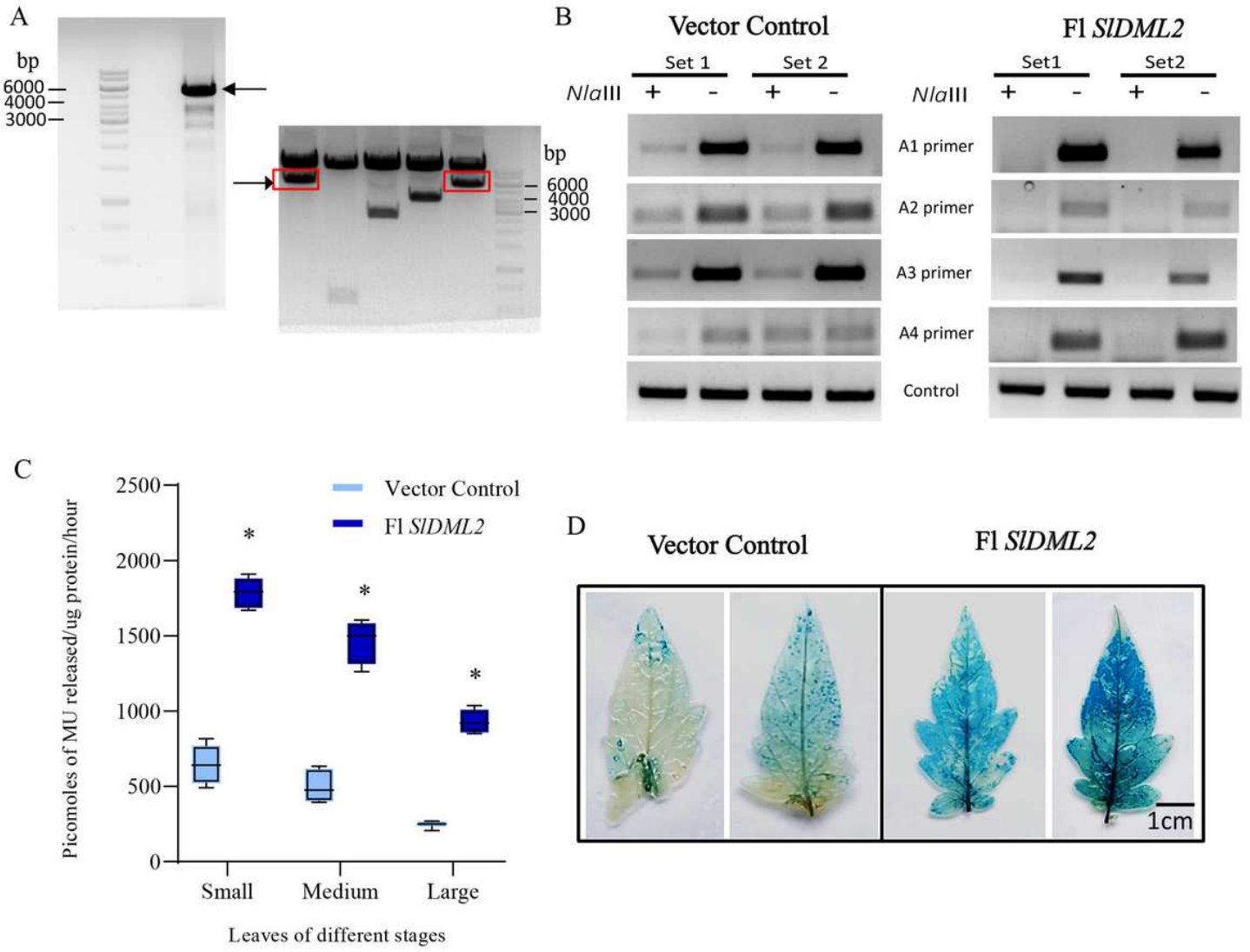

Figure 8

Restoration of promoter activity by DNA demethylase in mature leaves. A, Agarose gel photograph showing amplification and clone confirmation of SlDML2 full length(Fl) CDS(arrow). B, Agarose gel photograph showing resolved bands of methylation sensitive PCR amplicons in only vector and SlDML2 infiltrated transgenic tomato leaves. Amplification of a genomic region with no NlaIII sites used as loading control. C, MUG-assay data showing magnitude of SlTRN1 promoter activation upon full length SlDML2 infiltration in different sized leaves. D, GUS staining of vector and SlDML2 infiltrated transgenic mature tomato leaves. Intense staining upon SlDML2 expression confirmed reactivation of SlTRN1 promoter. *, significant change.

Supplementary Files

This is a list of supplementary files associated with this preprint. Click to download.

- ChowdhurySupplementaryFig1.pdf
- ChowdhurySupplementaryFig2.pdf
- ChowdhurySupplementaryFig3.pdf
- ChowdhurySupplementaryFig4.pdf
- ChowdhurySupplementaryTable1.pdf
- ChowdhurySupplementaryTable2.pdf
- ChowdhurySupplementaryTable3.pdf